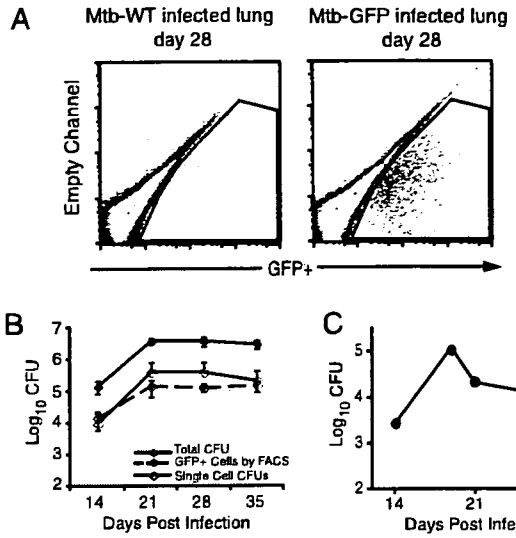

FIGURE 1. Flow cytometry detection of Mtb-GFP-infected cells from mouse lung tissues. *A*, Flow cytometry dot plots showing single-cell suspensions from the lungs of mice infected with wild-type Mtb H37Rv (Mtb-WT; *left panel*) or GFP-expressing Mtb H37Rv (*right panel*) 28 days postinfection, confirming that GFP^+ cells are only found in mice infected with Mtb-GFP. *B*, Quantitation of infection by comparison of the number of infected cells as determined by flow cytometry (—♦—) and bacterial CFU in total lung homogenate (—◇—) and in washed lung cells (- - -◇- - -). GFP^+ was calculated as the percentage of GFP^+ cells determined by flow cytometry multiplied by the total number of cells in the single-cell suspension. For total homogenate CFU, an aliquot of total disrupted lung tissue before any washing was serial diluted and plated on 7H11 agar in triplicate. For single-cell suspension CFU, an aliquot of the final single-cell preparation from the lung used to determine the total cell number was serial diluted without lysing the cells and plated on 7H11 agar in triplicate. Colonies were counted 14–21 days later. Data are the mean ± SD of five mice per time point. *C*, Bacterial load in the mediastinal lymph node was assessed by serial dilution of the total homogenate before any washing and plating on 7H11 agar from the experiment displayed in Fig. 3.

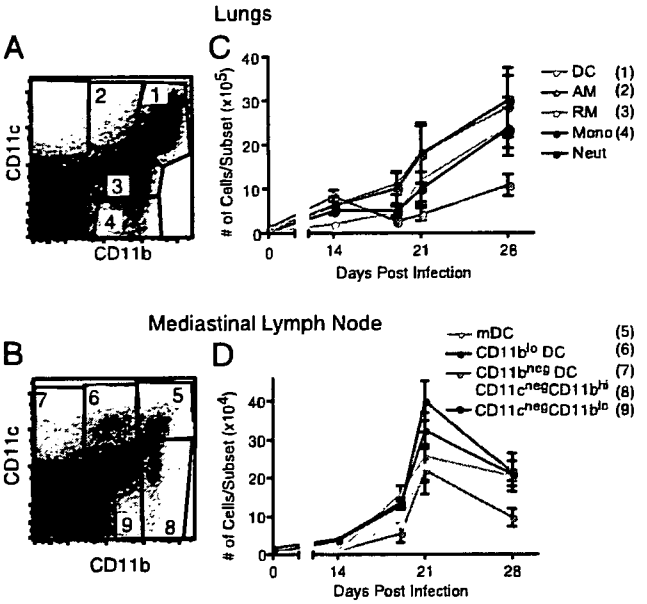

FIGURE 2. *A* and *B*, Flow cytometry dot plots of the distribution of CD11c- and CD11b-expressing cell subsets in the lungs (*A*) and the mediastinal lymph node (*B*) before (day 0) and after aerosol infection. *C* and *D*, The total number of cells in each of the CD11c/CD11b-defined subsets before (day 0) and during the course of infection in the lungs (*C*) and mediastinal lymph node (*D*). mDC, Myeloid DC; RM, recruited interstitial macrophage; AM, alveolar macrophage; Mono, monocyte; Neut, neutrophil. The neutrophil subset is not shown on the dot plot because it was excluded by gating on $CD11c^-Gr\text{-}1^{high}$ cells before identifying the CD11c/CD11b-defined subsets. Cell numbers were calculated by multiplying the percentage of cells in each subset obtained through flow cytometry by the total number of cells determined through manual count of the total number of cells in the single cell suspension from each tissue. Data are shown as mean ± SD for three (lymph nodes) or five (lungs) mice per time point. Cell populations in lungs of uninfected mice were ($\times 10^4$): myeloid DC, 2.2 ± 0.5; alveolar macrophage, 13 ± 3; recruited interstitial macrophage, 9.1 ± 2.1; monocytes, 5.3 ± 1.6; neutrophils, 1.9 ± 0.9. Cell populations in mediastinal lymph nodes of uninfected mice were ($\times 10^3$): myeloid DC, 4.1 ± 0.2; $CD11b^{low}$DC, 7.4 ± 0.1; $CD11b^-$DC, 2.5 ± 0.1; $CD11c^-CD11b^{high}$, 8.0 ± 0.2; $CD11c^-CD11b^{low}$, 18 ± 0.3.

medium (Molecular Probes) and visualized with a ×100 oil immersion objective on a Leica DMRB fluorescent microscope. Photomicrographs were recorded using a Spot Slider digital camera and Spot Software.

Stimulation of Mtb-specific $CD4^+$ T lymphocytes by cells from Mtb infected mice

T cells and B cells were removed from single cell suspensions of lungs and lymph node using Dynal magnetic bead selection (Invitrogen) to enrich for APCs. For live sorts, cells were stained in sterile PBS with 10% FCS, kept on ice, and sorted using a FACS Vantage at the New York University Center for AIDS Research. $CD4^+$ T cells were isolated from P25 TCR-Tg mice (21) by using a CD4 T cell isolation kit and an autoMACS system (Miltenyi Biotec). $CD4^+$ T cells ($1\text{–}2 \times 10^5$) were combined with sorted APCs at designated ratios in complete medium (RPMI 1640, 10% FCS, L-glutamine, nonessential amino acids, sodium pyruvate, HEPES, and 2-ME) in the presence of 10 μg/ml P25 TCR-specific peptide (Mtb Ag 85B aa 240–254, FQDAYNAAGGHNAVF; synthesized by Invitrogen Life Technologies) for 3 days at 37°C with 5% CO_2. Supernatants were assayed in triplicate for IFN-γ by ELISA (BD Biosciences).

CIITA-RAW264.7 cell Ag presentation assay

The FLAG epitope and open reading frame of human CIITA III were excised from p3FgCIITA8 (provided by Dr. J. Ting, University of North Carolina, Chapel Hill, NC) by using *Eco*RI and ligated into pQCXIN (Clontech Laboratories). The product was used to transfect GP2-293 cells, together with pVSV-G, to prepare vesicular stomatitis virus G protein-pseudotyped retroviral particles for the constitutive expression of CIITA and neo^r as a bicistronic message driven by the CMV immediate-early promoter with a viral internal ribosome entry site for the translation of neo^r. Packaged retroviral particles were used to transduce RAW264.7 cells, stably transduced cells were selected in G418, and individual clones were characterized by their levels of expression of surface MHC class II by FACS. A clone that expressed surface class II at a level that resembled that of mature bone marrow-derived DCs was expanded and used for subsequent studies.

For Ag presentation experiments, CIITA-RAW cells were grown in RPMI 1640 medium with 10% heat-inactivated FCS and 2 mM L-glutamine and plated at a density of 2.5×10^6 cells per 10-cm tissue culture dish. Mtb (H37Rv) was grown in Middlebrook 7H9 broth supplemented with ADC enrichment to an OD_{580} of 0.5–1.0. The culture was centrifuged at 2,200 × *g* for 10 min and the pellet was resuspended in 2 ml of RAW cell growth medium. Clumps of bacteria were disrupted by vortexing on high for 3 min in the presence of 3-mm glass beads and passed through a 5-μm syringe filter (Millipore) by gravity flow to remove clumps. Bacterial density was determined by counting in a Petroff-Hausser counter and confirmed by serial dilution and plating on 7H11 agar. CIITA-RAW cells were infected at a multiplicity of infection of 10 or treated with 200 ng/ml gamma-irradiated H37Rv for 18–24 h. CIITA-RAW cells were scraped and harvested in PBS with 5 mM EDTA and replated in a round-bottom 96-well plate at designated densities in triplicate in complete medium (RPMI 1640 medium, 10% heat-inactivated FCS, 10 mM HEPES, 100 μM nonessential amino acids, 1 mM sodium pyruvate, 100 U/ml penicillin, 100 μg/ml streptomycin sulfate, and 1× 2-ME). Cells were incubated with 1 μM OVA peptide (aa 323–339) (Peptides International) for 6 h and then fixed for 10 min with 1% paraformaldehyde and thoroughly washed with PBS. DO11.10 $CD4^+$ T cells that had been primed for 4 days in the presence of 1 ng/ml IL-12, 1 μM OVA peptide (323–339), and 10 μg/ml

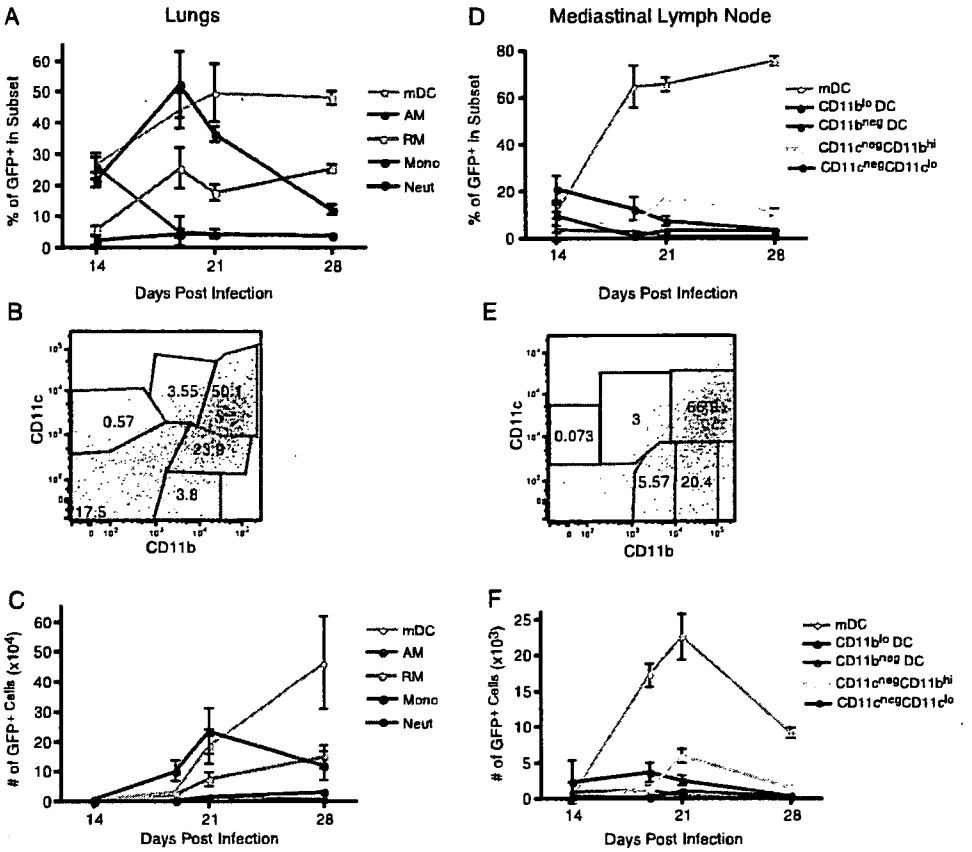

FIGURE 3. Distribution of Mtb-GFP infected cells in the CD11c/CD11b-defined leukocyte subsets of the lung and mediastinal lymph node. *A* and *D*, Percentage of GFP^+ cells that fall within each of the subsets of leukocytes in the lung (*A*) and mediastinal lymph node (*D*) during the course of infection. *B* and *E*, Flow cytometry dot plot of the distribution of GFP^+ cells in the lung (*B*) and mediastinal lymph node (*E*) at day 28 postinfection on a plot of CD11c vs CD11b. The gates represent the subsets of APCs identified in each tissue based on the surface expression of CD11c and CD11b. Fewer than 5% of the $CD11c^+$ cells in the lungs expressed either CD3 or CD8α, and Mtb-GFP were not detected in any $CD11c^+CD3^+$ or $CD11c^+CD8\alpha^+$ cells (not shown). The numbers in the gates represent the percentage of GFP^+ displayed in that gate. *C* and *F*, The total number of infected cells within the leukocyte subsets in the lung (*C*) and mediastinal lymph node (*F*) during the first 4 wk of infection. The total number of infected cells in each subset was determined by multiplying the percentage of the total cells that are GFP^+ within each subset as determined through flow cytometry by the total number of cells isolated from the tissue at each time point. Data shown are mean ± SD for five mice per time point. mDC, Myeloid DC; RM, recruited interstitial macrophage; AM, alveolar macrophage; Mono, monocyte; Neut, neutrophil.

anti-IL-4 were purified using a $CD4^+$ isolation kit and an autoMACS machine, added to the CIITA-RAW cells at 2×10^5 in complete medium, and incubated at 37°C and 5% CO_2 for two days. Supernatants were harvested and assayed in triplicate using ELISA with anti-mouse IFN-γ Abs (BD Biosciences), and absorbance was read on a microplate reader (Bio-Tek Instruments).

Statistical analysis

Statistical comparison of the number of bacteria per cell in myeloid DCs and recruited macrophages was performed by the Mann-Whitney *U* test and a comparison of the number of DCs and bacteria in lymph nodes of wild-type and *plt/plt* mice was performed by unpaired Students' *t* test, both using both Prism 4 for Macintosh (version 4.0a) from GraphPad Software.

Results

Flow cytometry detection of Mtb-infected cells from mouse tissues

To identify, characterize, and quantitate Mtb-infected cells in a temporal fashion during infection, we performed flow cytometry analysis on the lungs of mice infected with Mtb constitutively expressing GFP (Mtb-GFP). We first confirmed the specificity of detection by determining that green fluorescent events were detected in cells from mice infected with Mtb-GFP but not in cells from mice infected with wild-type Mtb (Fig. 1*A*). To confirm that

Table I. *Percentage of cells in each cell subset from the lungs that are GFP^+ over the course of infection*[a]

	Dendritic Cells	Alveolar Macrophages	Recruited Macrophages	Monocytes	Neutrophils
14	1.89 ± 0.99	0.77 ± 0.21	0.63 ± 0.28	0.11 ± 0.07	1.26 ± 0.77
19	10.14 ± 0.84	2.07 ± 0.36	4.88 ± 1.32	1.21 ± 0.41	9.09 ± 2.09
21	16.2 ± 1.82	4.09 ± 0.97	7.86 ± 2.71	2.76 ± 1.32	12.86 ± 3.62
28	15.63 ± 2.95	2.79 ± 0.4	6.82 ± 2.13	1.91 ± 0.43	3.52 ± 0.57

[a] Results shown are mean ± SD from analysis of five mice.

Table II. *Percentage of cells in each cell subset from the mediastinal lymph node that are GFP$^+$ over the course of infection*[a]

	Myeloid DC	CD11c$^+$CD11b^{low}	CD11c$^+$CD11b$^-$	CD11c$^-$CD11b^{high}	CD11c$^-$CD11b^{low}
14	2.83	1.51	1.69	1.17	0.13
19	8.22	0.40	0.15	0.87	0.0095
21	6.78	3.25	4.97	1.73	0.07
28	3.44	0.21	0.029	1.15	0.03

[a] Numbers were obtained by pooling cells from lymph nodes from five mice at each time point.

these green fluorescent events represented Mtb-GFP infected cells, we sorted cells in the positive and negative gates in the infected lung (Fig. 1*A*, *right panel*) and found that >90% of the cells in the positive gate contained one or more bacteria whereas <0.002% of the cells in the negative gate contained bacteria as detected by fluorescence microscopy.

We next monitored the numbers of Mtb-GFP$^+$ cells over several weeks of infection. First, we confirmed that the infection was progressing as expected by plating whole homogenates of total lung tissue for viable bacteria (Fig. 1*B*). We found the expected increase in bacterial counts from 14 to 21 days followed by a plateau in the number of bacteria. The number of fluorescent events per lung detected by flow cytometry displayed the same temporal pattern as the total bacterial counts (Fig. 1*B*). We consistently detected ~1 $\log_{10}$ fewer fluorescent events than viable bacteria (Fig. 1*B*). This difference is partially due to the loss of bacteria during the washing steps that were performed before FACS analysis as determined by assessing the CFU in the supernatant of each wash (data not shown). In addition, microscopic examination of sorted cells showed that many infected cells contained more than one bacterium (see below), resulting in a ratio of GFP$^+$ events to CFU of <1. Additionally, the number of fluorescent events detected correlated very closely with the number of viable bacteria detected in the washed, single-cell suspensions that were not lysed with detergent before plating (Fig. 1*B*). Taken together, these data indicate that our flow cytometry technique is both sensitive and specific for detecting infected cells and show that the number of infected cells first increases and then plateaus, mirroring the pattern of total bacterial counts. This indicates that during the initial phase of infection with Mtb before the appearance of the adaptive immune response, the growth of the bacterial population in the lungs is accompanied by an expansion of the number of infected cells, which implies a high rate of cell-to-cell spread of the bacteria. This cell-to-cell spread is diminished by the adaptive immune response, as the number of infected cells plateaus with the same kinetics as the bacterial population size.

Mtb infects lung cells with diverse phenotypes in vivo

Differential quantitative expression of the leukocyte markers CD11b and CD11c, together with bronchial lavage, identified three major and two minor subsets of myeloid cells in the lungs (15–17) (Fig. 2). At the earliest time point that Mtb-GFP could be reliably detected (14 days postinfection), alveolar macrophages, myeloid DCs, and neutrophils were the predominant infected cells in the lungs (Fig. 3). By 19 days postinfection myeloid DCs and interstitial macrophages were recruited to the lungs and outnumbered the alveolar macrophages (Fig. 2). Concurrent with their recruitment to the lungs, myeloid DCs and recruited interstitial macrophages became infected (Fig. 3) and were the predominant populations of infected cells in the lungs while alveolar macrophages, which changed minimally in total number during the course of infection, decreased as a fraction of the total infected cells in the lungs. We confirmed that GFP$^+$ cells in each of these cell subsets represented Mtb-infected cells by flow sorting of each subset, followed by examination of the sorted cells by fluorescence microscopy. Myeloid DCs and recruited macrophages remained the predominant infected cells in the lungs throughout the remainder of the monitored infection. Despite the long-standing belief that macrophages represent the resident cells for Mtb, myeloid DCs account for the largest percentage (>50%) of infected cells in the lung after 14 days of infection. Although recruited interstitial macrophages represent a significant percentage of the infected cells, infected myeloid DCs outnumber infected recruited macrophages by 2:1 at the peak of the infection in the lung (Fig. 3, *A* and *C*). Although accounting for approximately half the infected cells after 3 wk, the myeloid DCs only represent 6.8% of the total cells in the lung; therefore, a high proportion of the DCs in the lung become infected with Mtb (Tables I and II).

In addition to macrophages and DCs, between 14 and 21 days postinfection we found GFP$^+$ cells within a CD11c$^-$CD11b^{high}Gr-1^{high} population. Examination by microscopy of flow-sorted GFP$^+$ cells from this population confirmed that the GFP$^+$ cells contained Mtb, histological staining by Hema3 showed that 80% of the cells possessed granulocyte-like nuclei, and 72% of the cells were strongly positive for myeloperoxidase activity by Leder stain. Taken together, these results indicate that granulocytes are transiently infected with Mtb early in infection but that they represent a minor fraction of the infected cells at later times.

DCs transport Mtb to the mediastinal lymph node

We also used flow cytometry to characterize the cells in the mediastinal lymph node, which drains the lungs. After day 14 postinfection, one population of cells dominated the distribution of infected cells in the mediastinal lymph node (Fig. 3, *D–F*). Greater than 65% of the infected cells were CD11c^{high}CD11b^{high} myeloid DCs, which resemble the predominant infected cell population in the lungs. The total number of these cells increased progressively in the lymph node during the course of infection (from 1×10^4 to

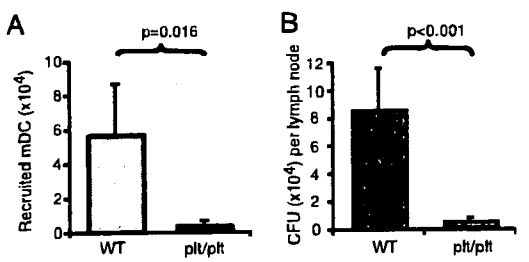

FIGURE 4. DCs and Mtb CFU in lymph nodes of C57BL/6J and *plt/plt* mice 14 days after aerosol infection with ~100 Mtb CFU/mouse. *A*, Recruitment of myeloid DCs, calculated as the increase in myeloid DCs in the mediastinal lymph node in response to Mtb infection of wild-type and *plt/plt* mice relative to the number of myeloid DCs in uninfected lymph nodes from each strain of mice. *B*, Mtb CFU in the mediastinal lymph node. Data represents the mean ± SD of at least five mice in each group. WT: Wild-type C57BL/6 mice.

Table III. *APC subsets in mediastinal lymph nodes of wild-type and plt/plt mice before and 14 days after M. tuberculosis infection*[a]

	C57BL/6				*plt/plt*			
	Uninfected		Day 14		Uninfected		Day 14	
Cell Subset	Percentage (%)	$\times 10^4$	Percentage (%)	$\times 10^4$	Percentage (%)	$\times 10^4$	Percentage (%)	$\times 10^4$
Total Cells		182		950		50		54.8
Total APC	7.91	14.4 ± 0.4	4.7	44.8 ± 22.5	5.43	2.72	7.76	4.2 ± 2.1
Myeloid DC	0.83	1.5 ± 0.1	0.54	4.9 ± 3.8	0.57	0.29	0.95	0.5 ± 0.4
CD11b^{low} DC	1.48	2.7 ± 0.02	0.96	9.4 ± 5.6	0.61	0.31	1.36	0.7 ± 0.4
CD11b$^-$ DC	0.49	0.9 ± 0.05	1.04	9.9 ± 6.7	0.55	0.28	2.32	1.2 ± 1.0
CD11c$^-$CD11b^{high}	1.59	2.9 ± 0.1	0.56	5.1 ± 2.9	1.56	0.78	0.75	0.42 ± 0.3
CD11c$^-$CD11b^{low}	3.52	6.4 ± 0.2	1.6	15.4 ± 8.5	2.15	1.08	2.38	1.3 ± 0.7

[a] Data from uninfected *plt* mice were obtained by pooling cells from lymph nodes of five mice; the remaining data are mean ± SD of five mice per group.

2×10^5), and by day 19 ~25% of these cells in the mediastinal lymph node contained bacteria detectable by flow cytometry. In contrast to the total number of myeloid DCs in the mediastinal lymph node, the number of infected myeloid DCs reached a peak of $\sim 2.5 \times 10^4$ by day 21 postinfection and then decreased to $\sim 8 \times 10^3$ per lymph node by day 28. The number of viable bacteria in the lymph node decreased by a similar extent between days 21 and 28.

Infected lymph node cells could arise by several different mechanisms, including the drainage of cell-free bacteria from the lungs in lymphatic fluid, the phagocytosis of hematogenously spread bacteria by resident cells in the lymph node, or the transport by DCs that become infected in the lungs and then migrate to the lymph node when they mature. To distinguish these possibilities we infected *plt* mice that lack the expression of CCL19 and CCL21ser (22), which are normally expressed in the lymphatic endothelium and the paracortical zone of lymph nodes and serve as ligands for CCR7 on mature DCs. Compared with wild-type controls, mediastinal lymph nodes of *plt* mice recruited 95% fewer CD11c^{high}CD11b^{high} cells and contained 95% fewer bacteria on day 14 after Mtb infection (Fig. 4). The number of lung DCs or macrophages and the number of bacteria in the lungs did not differ significantly on day 14 between *plt* mice and controls. Although the recruitment of other APC subsets to the mediastinal lymph node was also defective in Mtb-infected *plt* mice (Table III), the defective migration of myeloid DCs is most likely to account for the lower number of bacteria in the lymph node because this subset represents the largest fraction of infected cells in the lymph node. These results support the hypothesis that mature DCs transport live Mtb from the lungs to the local draining lymph node, at least during the early phase of infection. The observation that the number of Mtb-infected myeloid DCs in the lymph node decreases later in infection while the number of infected myeloid DCs in the lungs remains at the high level achieved by day 21 (Fig. 3) implies that migration of Mtb-infected myeloid DCs from the lungs to the mediastinal lymph node is a transient phenomenon and is down-regulated in the later stages of infection.

Immunohistochemistry localizes Mtb in DEC-205$^+$ cells

As an alternative approach to determining the frequency of Mtb infection of DCs, we used immunohistochemistry and a well-characterized Ab to the DC marker DEC-205. Because immunohistochemistry staining and acid-fast staining of mycobacteria are incompatible, we performed these studies using a strain of Mtb transformed with a plasmid for constitutive expression of *Escherichia coli* β-gal. This revealed that bacteria could be detected in DEC-205$^+$ as well as DEC-205$^-$ cells in pulmonary granulomas and that infected DEC-205$^+$ cells formed aggregates with other infected DEC-205$^+$ cells while infected DEC-205$^-$ cells clustered with other DEC-205$^-$ cells (Fig. 5). When we quantitated the frequency of Mtb in DEC-205$^+$ cells in the lungs we found that 21 days after infection 53% of the bacteria were in DEC-205$^+$ cells; this increased to 63% by 28 days after infection. These results support the observations obtained by flow cytometry that the majority of bacteria reside in lung cells with the characteristics of DCs.

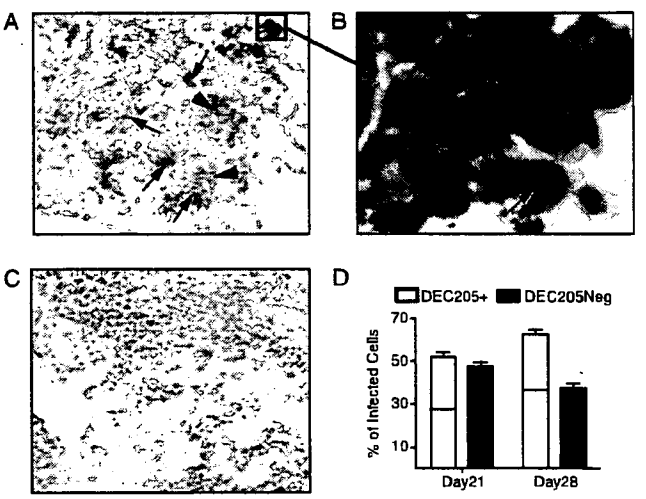

FIGURE 5. Immunohistochemical localization of Mtb in DEC-205$^+$ and DEC-205$^-$ lung cells. Mtb-β-gal was visualized with X-galactosidase (blue-green) and DEC-205 (red) was visualized with the mAb NLDC-145 in hematoxylin-counterstained (blue) lung sections from a mouse infected by the aerosol route 28 days earlier. *A*, Original magnification: ×20; arrows designate bacteria in DEC-205$^+$ cells and arrowheads designate bacteria in DEC-205$^-$ cells. *B*, Original magnification: ×100 with oil immersion. *C*, Isotype control stained lung, counterstained with hematoxylin. *D*, On days 21 and 28 postinfection Mtb-β-gal was scored for its localization in DEC-205$^+$ or DEC-205$^-$ cells in lung sections. DEC-205$^+$ cells were further categorized as staining with high (*lower section* of bar) or low (*upper section* of bar) intensity. At each time point the distribution of Mtb-β-gal was determined in cells on six lung sections; the percentage of bacteria in DEC205$^+$ and DEC-205$^-$ cells was calculated for each section; data shown are mean ± SD for the six sections from each time point. On sections from day 21, a total of 525 Mtb-β-gal$^+$ cells were counted; on sections from day 28, a total of 722 Mtb-β-gal$^+$ cells were counted.

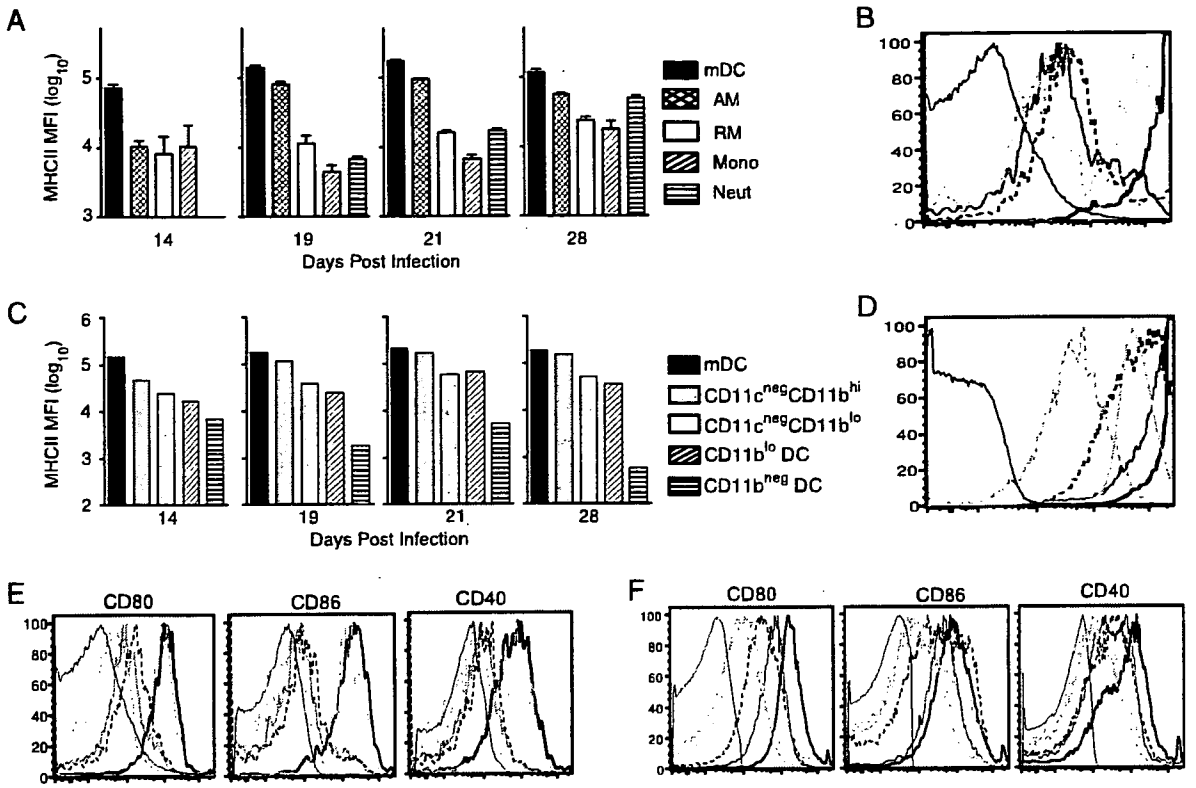

FIGURE 6. Expression of surface MHC class II on Mtb-GFP-infected cells in the CD11c/CD11b-defined subsets of leukocytes in the lung and mediastinal lymph node. *A*, MHC class II mean fluorescence intensity of the GFP$^+$ cells within each cell subset during the first 4 wk of infection. Data shown are mean ± SD for five mice per time point. mDC, Myeloid DC; RM, recruited interstitial macrophage; AM, alveolar macrophage; Mono, monocyte; Neut, neutrophil. *B*, Histogram of MHC class II expression on lung cell subsets from a representative mouse 21 days postinfection. Bold black line, Myeloid DC; dark gray line, alveolar macrophage; light gray line, recruited interstitial macrophage; dashed gray line, monocyte; heavy dashed line, neutrophil; fine black line, control. *C*, MHC class II MFI for the GFP$^+$ cells within each of the CD11c/CD11b-defined cell subsets in the mediastinal lymph node. Cells from the mediastinal lymph nodes of five mice per time point were pooled into a single sample to acquire sufficient GFP$^+$ events for quantitation. *D*, Histogram of MHC class II expression on lymph node cell subsets from a representative mouse 21 days postinfection. Bold black line, Myeloid DC; heavy dashed line, CD11b^{low} DC; dashed gray line, CD11b$^-$ DC; dark gray line, CD11c$^-$CD11b^{high}; light gray line, CD11c$^-$CD11b^{low}; fine black line, control. *E* and *F*, Representative histograms of costimulatory molecule expression on each APC subset from the lung (*E*) and mediastinal lymph node (*F*) 21 days postinfection. Cell subsets are designated as in *B* and *D*. Expression of MHC class II on all CD11c/CD11b-defined subsets in the lungs and lymph nodes of uninfected mice was below the lower limit of the scale shown in *A* and *C*.

APCs in the lungs and mediastinal lymph nodes of Mtb-infected mice express surface MHC class II and costimulatory molecules

Secondary lymphoid tissues such as lymph nodes are the sites of the priming of naive CD4$^+$ T lymphocytes by MHC class II-restricted recognition of peptide Ag, usually on DCs. In the lungs, Ag presentation is necessary for recognition of infected cells by Mtb Ag-specific effector CD4$^+$ T cells. Our finding that Mtb infects DCs in the lungs and mediastinal lymph node indicates that these cells contain Mtb Ag and may participate in the activation of naive (lymph node) and effector (lung) CD4$^+$ T cells. We found that myeloid DCs from the lungs and the mediastinal lymph nodes of Mtb-infected mice expressed high levels of MHC class II (Fig. 6). DCs in the lungs of infected mice expressed progressively higher levels of surface MHC class II from 14 to 21 days after infection, consistent with progressive maturation of resident and newly recruited DCs by bacterial products and by proinflammatory cytokines induced by infection (23, 24). Likewise, myeloid DCs in the mediastinal lymph node expressed high levels of MHC class II, consistent with maturation. Further evidence for the maturation of DCs in the lungs and mediastinal lymph node was provided by the expression of costimulatory molecules (CD80, CD86, and CD40) on a higher proportion of lung and mediastinal lymph node DCs

Table IV. *Percentage of GFP$^+$ cells in each lung cell subset that express costimulatory molecules*[a]

	CD86			CD80		CD40	
Subset	Day 14	Day 21	Day 28	Day 14	Day 28	Day 14	Day 28
Myeloid DC	73.8 ± 7.32	91.6 ± 1.38	53.9 ± 1.82	97.4 ± 2.78	83.3 ± 1.78	40.8 ± 9.65	72.1 ± 3.07
Alveolar Macrophage	35.5 ± 8.94	92.8 ± 0.96	74 ± 6.48	94.1 ± 3.91	86.3 ± 2.03	6.68 ± 2.56	73.5 ± 8.29
Recruited Macrophage	51.7 ± 18.3	27 ± 3.7	28.9 ± 3.36	71 ± 14.1	47.8 ± 5.51	36.1 ± 13.7	21.1 ± 3.88
Monocyte	17.9 ± 12.5	13.9 ± 2.31	8.29 ± 2.33	38.8 ± 38.8	16.5 ± 7.24	17.35 ± 4.85	3.19 ± 0.4
Neutrophil	78.3 ± 6.95	27.4 ± 2.56	9.87 ± 1.94	89.5 ± 7.74	21.8 ± 3.29	75.6 ± 3.63	15.2 ± 3.04

[a] Results shown are mean ± SD from analysis of five mice at each time point.

Table V. *Percentage of total (GFP$^+$ and GFP$^-$) lung cells in each subset that express costimulatory molecules*[a]

Subset	CD86			CD80		CD40	
	Day 14	Day 21	Day 28	Day 14	Day 28	Day 14	Day 28
Myeloid DC	62.3 ± 5.64	85.1 ± 3.48	65.4 ± 1.64	54.4 ± 20.9	83.1 ± 1.08	32.4 ± 10.1	57.2 ± 1.38
Alveolar Macrophage	36.9 ± 4.24	88.9 ± 1.52	71.1 ± 2.64	80.7 ± 10.4	87.5 ± 0.64	3.33 ± 2.23	27.2 ± 3.17
Recruited Macrophage	41.2 ± 5.82	45 ± 4.66	28.1 ± 4.48	62.4 ± 9.3	46.8 ± 3.5	33.9 ± 2.79	11.9 ± 0.39
Monocyte	19.4 ± 5.94	31 ± 2.06	13.8 ± 2.27	27.7 ± 10.5	23.3 ± 3.61	7.24 ± 2.52	3.5 ± 0.44
Neutrophil	76.1 ± 5.99	33.7 ± 4.26	6.67 ± 0.91	87.7 ± 5.06	11.7 ± 1.41	73.1 ± 3.63	3.18 ± 0.34

[a] Results shown are mean ± SD from analysis of five mice at each time point.

(Tables IV and V). Consistent with other studies in mice (15) and humans (25), we found that alveolar macrophages also expressed high levels of MHC class II, although the levels were not as high as those on DCs. By comparison, newly recruited interstitial macrophages, which represent a major subset of the Mtb-infected cells in the lungs, expressed lower levels of MHC class II as reflected by 10-fold lower fluorescence intensity by flow cytometry, and a lower proportion of these cells expressed CD80 and CD86 (Fig. 6 and Tables IV and V).

Subsets of cells from tissues of Mtb-infected mice differ in their ability to stimulate Mtb-specific CD4$^+$ T lymphocytes

The differences in expression of MHC II and costimulatory molecules on distinct subsets of cells from Mtb-infected mice suggested that cells in the subsets might differ in their capacity to stimulate CD4$^+$ T lymphocytes. To test this hypothesis, we sorted lung and mediastinal lymph node cells on the basis of their quantitative expression of CD11b and CD11c and used the sorted cells to stimulate T cell Ag receptor (TCR) Tg (P25 TCR-Tg) CD4$^+$ T cells that recognize a peptide from Mtb Ag 85B (21).

In the lymph node, we expected that the myeloid DCs from Mtb-infected mice would be the most efficient APCs to CD4$^+$ T cells because they exhibit a mature phenotype and are well known for their efficiency as APCs. However, we found that myeloid DCs from mediastinal lymph nodes of Mtb-infected mice were poorer APCs than were CD11c^{high}CD11b$^{low/-}$ DCs, which elicited twice as much IFN-γ from the responding T cells as than did myeloid DCs (Fig. 7*A*). The same pattern was observed for the stimulation of IL-2 secretion, indicating that the differential ability of the APC subsets was not confined to a single T cell response (not shown). When we compared the ability of the same subsets of DCs (after maturation with TNF and LPS) from lymph nodes of uninfected mice to stimulate P25 TCR-Tg cells, myeloid DCs were the most efficacious in stimulating the production of IFN-γ from the responding T cells (data not shown). Because myeloid DCs are the predominant Mtb-infected cells in the lymph node and nonmyeloid DCs are infected with very low frequency, these results suggest that Mtb infection may inhibit direct Ag presentation by myeloid DCs.

Among the cells in the lungs, we also anticipated that myeloid DCs would be efficient APCs because they express the highest levels of surface MHC class II and costimulatory molecules. However, as in the mediastinal lymph nodes, myeloid DCs isolated from the lungs stimulated P25 TCR-Tg CD4$^+$ cells poorly. Indeed, myeloid DCs isolated from the lungs of Mtb-infected mice stimulated the CD4$^+$ T cells no more effectively than did recruited macrophages, which express lower levels of MHC II and costimulatory molecules (Fig. 7*B*). In contrast, alveolar macrophages, which represent a small percentage of the total of the infected cells, consistently elicited the greatest amount of IFN-γ from P25 TCR-Tg CD4$^+$ T cells. In comparison to mediastinal lymph node cells with comparable surface phenotypes, all of the subsets of cells from the lungs were less efficacious stimulators of CD4$^+$ T cells.

Mtb inhibits MHC class II Ag presentation without reducing surface class II expression

The finding that cells from Mtb-infected mice were poor stimulators of Ag-specific CD4$^+$ T cells suggested that Mtb infection might inhibit class II Ag presentation. To test this hypothesis, we constructed a cell line that constitutively expresses high levels of surface MHC class II and other mediators of class II Ag presentation due to the constitutive expression of CIITA. These cells were efficient APCs to DO11.10 OVA-specific TCR-Tg CD4$^+$ T lymphocytes (Fig. 8). When these cells were infected with live, virulent Mtb, their stimulation of DO11.10 cells was reduced by 90% without a significant change in their surface expression of

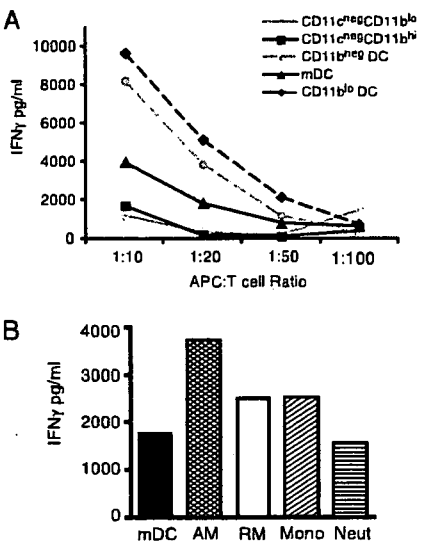

FIGURE 7. Ag-specific CD4$^+$ T lymphocyte-stimulating capacity of CD11c/CD11b-defined cell subsets from lungs and mediastinal lymph nodes of Mtb-infected mice. *A*, Cells in each of the CD11c/CD11b-defined subsets in the mediastinal lymph node of mice infected 28 days earlier were sorted by FACS and combined with Mtb Ag85B-specific transgenic CD4$^+$ T lymphocytes (P25 TCR-Tg) at the designated ratios in the presence of antigenic peptide. Three days later supernatants were assayed for the presence of IFN-γ to assess T cell activation. mDC, myeloid DC. *B*, Cells in each of the CD11c/CD11b-defined subsets from the lungs of mice infected for 28 days were sorted by FACS and combined with P25 TCR-Tg CD4 T cells at 1:10 APCs to T cells. After a three-day incubation, supernatants were assayed for IFN-γ. Graphs are representative of five independent experiments with each tissue. mDC, Myeloid DC; RM, recruited interstitial macrophage; AM, alveolar macrophage; Mono, monocyte; Neut, neutrophil.

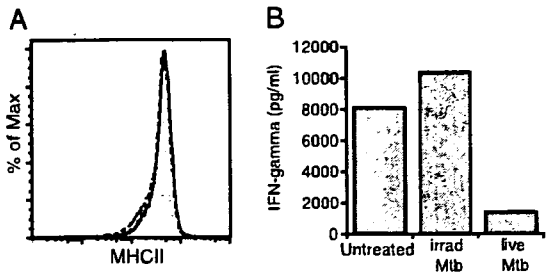

FIGURE 8. Inhibition of Ag presentation by Mtb in vitro. *A*, Histogram of surface expression of MHC class II on the clone of CIITA-RAW cells used for Ag-presentation experiments. Shaded area, Untreated CIITA-RAW cells; dashed line, CIITA-RAW cells exposed to gamma-irradiated Mtb; dotted line, CIITA-RAW cells infected with live Mtb. *B*, CIITA-RAW cells were exposed to gamma-irradiated (irrad) or live Mtb or medium alone and assayed for their ability to present OVA peptide (325–339) to Th1-polarized DO11.10 T cells, assayed as the production of IFN-γ after 48 h. The results shown are representative of four independent experiments.

MHC class II or a reduction in the surface expression of CD80 or CD86. Inhibition of Ag presentation by the CIITA-RAW cells required live Mtb, as no effect was observed when the cells were treated with gamma-irradiated Mtb.

Inefficient CD4$^+$ T cell stimulation is accompanied by the accumulation of intracellular bacteria in lung DCs and recruited macrophages

CD4$^+$ T cells provide protection against progressive growth of Mtb by secreting TNF and IFN-γ and by incompletely characterized cell contact-dependent mechanisms (26–28). The observation that Mtb-infected recruited interstitial macrophages and myeloid DCs were poorly recognized by Mtb-specific CD4$^+$ T cells suggests that these cells would be permissive for intracellular growth of Mtb in vivo. To test this hypothesis, we counted the number of bacteria per cell after sorting GFP$^+$ myeloid DCs and recruited macrophages from the lungs (Fig. 9). Accurate enumeration of the number of bacteria per cell was only possible at low cellular bacterial densities, so we used a conservative cutoff and scored all cells with five or more bacteria as having five bacteria per cell. Despite this conservative cutoff, we found that lung DCs contained 3.76 ± 0.05 bacteria per cell, whereas recruited macrophages contained 4.13 ± 0.05 bacteria/cell ($p = 0.0001$, by Mann-Whitney U test). Moreover, while 32% of infected lung DCs contained at least five bacteria per cell, nearly twice as many infected recruited macrophages (59%) contained at least five bacteria per cell and many of the macrophages were densely packed with bacteria, whereas few densely infected DCs were found (Fig. 9). These findings indicate that multiple subsets of APCs are permissive for the growth of Mtb in vivo and that cells that stimulate Ag-specific CD4$^+$ T cells poorly contain more bacteria per cell.

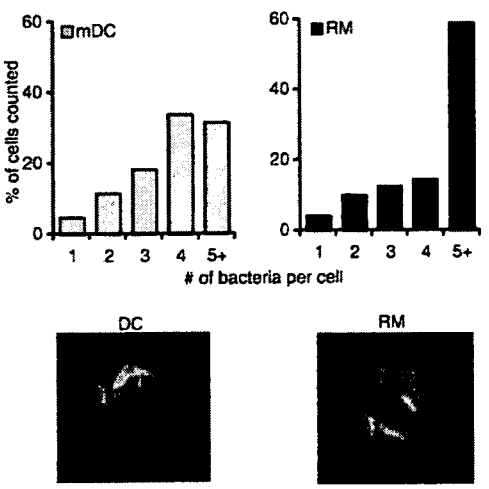

FIGURE 9. Frequency distribution of the number of Mtb-GFP per cell in recruited macrophages (RM)and DCs isolated from lungs (day 21 postinfection). GFP$^+$ recruited macrophages and DCs were sorted by FACS and nuclei were visualized with 4′,6′-diamidino-2-phenylindole. Approximately 450 cells of each type were examined by fluorescent microscopy and the number of bacteria in each cell was assessed visually, with all cells that contained at least five bacteria per cell counted as "5+." Micrographs show representative cells from the DC 5+ bacteria per cell group and the recruited macrophage 5+ bacteria per cell group. mDC, myeloid DC.

Discussion

The studies reported here reveal several major findings regarding the early stages of infection and the adaptive immune response after aerosol infection with Mtb. First, they demonstrate that Mtb infects cells of diverse phenotypes, that the predominant infected cell populations change with time, and that myeloid DCs are one of the major cell populations that are infected with Mtb in the lungs and lymph nodes. Second, we found that the population of Mtb-infected cells in the lung-draining lymph node is much less diverse than that in the lungs; up to 80% of the bacteria in the lymph node are found in myeloid DCs. Moreover, we found evidence that the bacteria in the lung-draining lymph node are transported there from the lungs by a CCL19/21-dependent mechanism and that the transport of bacteria to the lymph node is a transient phenomenon. Third, we found that the lymph node cell subsets that are most efficacious in presenting an Mtb peptide Ag to CD4$^+$ T lymphocytes are not infected with the bacteria and are not represented in the lungs of infected mice. Finally, we found that the cell populations that are infected with Mtb at high frequency are relatively ineffective at stimulating Ag-specific CD4$^+$ T cells, and we have obtained evidence that live Mtb can inhibit MHC class II Ag presentation without a decrease in the surface expression of MHC class II.

Since 1925, mononuclear phagocytes have been known to be resident cells for Mtb in vivo (11). Until recently, Mtb has been thought to reside exclusively in macrophages, although recent studies have detected bacteria in DCs in tissues of mice and humans (12, 13, 29). The sensitive and specific flow cytometry assay we have developed has allowed us to detect and characterize cells infected with GFP-expressing Mtb and to find that the cell populations that contain Mtb during the initial 4 wk of infection are highly dynamic and that DCs, not macrophages, are the quantitatively predominant subset of the infected cells in the lungs after the first 2 wk of infection. In the studies reported here, lung DCs were identified by their high-level expression of both CD11c and CD11b as previously described (15–17). In addition, we found that this cell subset in the lungs exhibits other characteristics of DCs, including IFN-γ-independent expression of high levels of surface MHC class II and high levels of the costimulatory molecules CD80 and CD86. This same subset of cells in the lungs has been found by other investigators to exhibit additional properties of DCs, including characteristic morphology in situ (17), the ability to migrate from the lungs to the mediastinal lymph node (16, 30), and the ability to prime naive T cells (16, 17). Moreover, we found that a large fraction of the infected cells in the lungs express the DC marker DEC-205 as determined by immunohistochemistry. Although our findings indicate that lung DCs are a major cell subset

infected with Mtb, they do not establish whether the infected cells exhibited a DC phenotype before infection or whether a subset of macrophages undergoes a transition to a DC phenotype in response to Mtb infection.

The number of DCs and recruited macrophages in the lungs increases progressively during the first 4 wk of infection, at least in part due to CCR2-dependent signaling (31–33), and upon arrival in the lungs the DCs and recruited macrophages become infected and markedly outnumber the initially infected alveolar macrophages, which do not change in total number or the number of infected cells after the first 2 wk of infection. After the 3rd wk of infection, newly recruited DCs and macrophages together account for 80–90% of the infected cells in the lungs, and afterward the distribution of the bacteria in these cells remains stable. Between days 14 and 19 postinfection, concurrent with DC recruitment and infection in the lungs, DCs mature as assessed by expression of surface MHC class II and the costimulatory molecules CD80 and CD86. Within this same interval, infected DCs transport live Mtb from the lungs to the lung-draining mediastinal lymph node, which indicates that at least a subset of infected lung DCs express CCR7, CCR8, and/or other chemokine receptors required for migration, at least in the first 14–17 days of infection.

Within the lung-draining mediastinal lymph node, all of the subsets of cells defined by the expression of CD11b and CD11c increased in number by day 19 of infection, and all of them stayed persistently increased in number compared with that in uninfected mice for at least the first four weeks of infection. Of the lymph node cells that contained Mtb, up to 80% are $CD11c^{high}CD11b^{high}$ myeloid DCs, which implies that only this subset of cells, and neither of the macrophage subsets, is capable of migrating from the lungs to the lymph node, consistent with the results observed after the administration of fluorescent latex particles (16) or infection with an influenza virus (30). The number of Mtb-infected DCs in the lymph node reached a peak on day 21 after infection, when the number of DCs containing bacteria in the lungs also reached its maximum level. On day 21, the number of Mtb-infected myeloid DCs in the lymph node was ~10% of the number in the lungs, which suggests that during the initial weeks of infection a high proportion of the DCs in the lungs that become infected migrate from the lungs to the local lymph node. Unlike the pattern seen in the lungs, the number of infected myeloid DCs in the lymph node decreases markedly after day 21, so that by day 28 the number of infected cells in the lymph node is only 2% of that in the lungs. One potential explanation for this finding is that infected DCs stop migrating from the lungs to the lymph node, as has been observed for lung DCs after infection with an influenza virus (30). However, this is not likely to be the sole explanation, because the total number of myeloid DCs in the lymph node remains stable from days 19–28. An additional possibility is that total DC migration from the lungs does not cease but that migration of Mtb-infected DC is selectively arrested after days 17–21. Further studies will be required to determine whether selective differences in the migration of Mtb-infected and uninfected lung DCs occurs after an initial wave of migration of infected lung DCs. The finding that DC migration from the lungs to the lymph node is temporally restricted despite chronic infection implies that Mtb Ags that are only expressed during the later stages of infection may not be efficiently presented to naive T lymphocytes.

Because myeloid DCs are the predominant population of cells that contain Mtb in the mediastinal lymph node, we expected that they would also exhibit the highest capacity for Ag presentation to Mtb-specific $CD4^+$ T lymphocytes. Instead, the $CD4^+$ T cell stimulating capacity of myeloid DCs from the mediastinal lymph node was exceeded by that of two alternative populations of lymph node DCs that expressed low or negligible levels of CD11b. Because neither of these cell populations is infected at high frequency in vivo and because neither is found in the lungs, our results suggest that while myeloid DCs transport live Mtb from the lungs to the lymph node, the priming of naive Mtb-specific $CD4^+$ T lymphocytes may be accomplished by resident lymph node DCs as has been reported during the early immune response to *Leishmania major* after intradermal infection (34). Further studies will be necessary to determine the precise mechanism(s) of the presentation of Mtb Ags to naive $CD4^+$ T lymphocytes, including the quantitative roles of Ag produced by bacteria in the lungs or in the lymph node and the quantitative contributions of Ags acquired by DCs from apoptotic macrophages.

When we examined the Ag presentation capacity of DCs and macrophages isolated from the lungs of infected mice, we found that they were less able to stimulate Mtb Ag85B-specific $CD4^+$ T lymphocytes than were lymph node cells. Myeloid DCs from the lungs stimulated Mtb-specific $CD4^+$ T cells to secrete approximately half the amount of IFN-γ observed when DCs from the lymph node were used despite comparable levels of expression of surface MHC class II, CD80, CD86, and CD40. These results indicate that the DCs found in the lungs are less efficacious APCs than those in the lymph node. One possible explanation is that Mtb-infected lung DCs undergo a defective maturation program that limits their capacity to migrate to lymph nodes as well as to present peptide Ags by the class II pathway. Indeed, Mtb has been reported to inhibit the maturation of human peripheral blood-derived DCs in vitro (35), but the results reported here are the first to demonstrate that this phenomenon also occurs in vivo.

To seek evidence that Mtb inhibits MHC class II Ag presentation in cells that do not require treatment with IFN-γ for class II expression, we constructed a macrophage cell line that constitutively expresses CIITA, which drives high levels of surface class II. Using those cells, we found that live, but not gamma-irradiated, Mtb inhibits class II Ag presentation to $CD4^+$ T lymphocytes despite abundant surface class II. This cell line should prove valuable for studies of the cellular basis of the inhibition of class II Ag presentation and for screening libraries of mutant Mtb to identify bacterial mechanisms of inhibiting Ag presentation.

In addition to the poorer Ag-presenting capacity of DCs from the lungs compared with that of DCs from the lymph node, recruited lung macrophages exhibited even lower efficacy in stimulating Mtb Ag85B-specific $CD4^+$ T lymphocytes. This was accompanied by a lower surface expression of MHC class II and in the presence of a lower frequency of expression of CD80 and CD86 in recruited macrophages compared with that in lung DCs. That this may have functional relevance is indicated by our finding that recruited macrophages contain significantly more bacteria per cell than do DCs in the lungs, although from these experiments it is not possible to determine whether the greater number of bacteria is the cause or the effect of poor Ag presentation and T cell stimulation.

In summary, we have found that Mtb infects phagocytes with diverse phenotypes in vivo and that myeloid DCs transport Mtb from the lungs to the local lymph node during the early, but not later, stages of infection. Moreover, we have found that DCs and recruited macrophages in the lungs are poor stimulators of Mtb Ag-specific $CD4^+$ T cells. Taken together, these results imply that vaccines that induce cellular immune responses to Mtb Ags may have limited efficacy if the responding memory and effector T lymphocytes cannot effectively recognize infected lung cells. In addition to ongoing vaccine development, efforts to develop strategies for overcoming immune evasion by Mtb need to be a high priority.

Acknowledgments

We thank the staff of the Gladstone Institute Flow Cytometry Core for assistance with flow cytometry optimization, the staff of the New York University Center for AIDS Research for assistance with cell sorting, and Wendy Peters, Ph.D., for assistance during early stages of this work.

Disclosures

The authors have no financial conflict of interest.

References

1. Mogues, T., M. E. Goodrich, L. Ryan, R. LaCourse, and R. J. North. 2001. The relative importance of T cell subsets in immunity and immunopathology of airborne *Mycobacterium tuberculosis* infection in mice. *J. Exp. Med.* 193: 271–280.
2. North, R. J., and Y. J. Jung. 2004. Immunity to tuberculosis. *Annu. Rev. Immunol.* 22: 599–623.
3. Sonnenberg, P., J. R. Glynn, K. Fielding, J. Murray, P. Godfrey-Faussett, and S. Shearer. 2005. How soon after infection with HIV does the risk of tuberculosis start to increase? A retrospective cohort study in South African gold miners. *J. Infect. Dis.* 191: 150–158.
4. Opie, E., and J. Aronson. 1927. Tubercle bacilli in latent tuberculous lesions and in lung tissue without tuberculous lesions. *Arch. Pathol. Lab. Med.* 4: 1–21.
5. Robertson, H. 1933. The persistence of tuberculous infections. *Am. J. Pathol.* 9: 711–719.
6. Wang, C. 1917. An experimental study of latent tuberculosis. *Lancet* 2: 417–419.
7. Perlman, D. C., W. M. el-Sadr, E. T. Nelson, J. P. Matts, E. E. Telzak, N. Salomon, K. Chirgwin, and R. Hafner. 1997. Variation of chest radiographic patterns in pulmonary tuberculosis by degree of human immunodeficiency virus-related immunosuppression: The Terry Beirn Community Programs for Clinical Research on AIDS (CPCRA), the AIDS Clinical Trials Group (ACTG). *Clin. Infect. Dis.* 25: 242–246.
8. Shafer, R. W., A. B. Bloch, C. Larkin, V. Vasudavan, S. Seligman, J. D. Dehovitz, G. DiFerdinando, R. Stoneburner, and G. Cauthen. 1996. Predictors of survival in HIV-infected tuberculosis patients. *AIDS* 10: 269–272.
9. Cooper, A. M., D. K. Dalton, T. A. Stewart, J. P. Griffin, D. G. Russell, and I. M. Orme. 1993. Disseminated tuberculosis in interferon γ gene-disrupted mice. *J. Exp. Med.* 178: 2243–2247.
10. Flynn, J. L., J. Chan, K. J. Triebold, D. K. Dalton, T. A. Stewart, and B. R. Bloom. 1993. An essential role for interferon γ in resistance to *Mycobacterium tuberculosis* infection. *J. Exp. Med.* 178: 2249–2254.
11. Cunningham, R. S., F. R. Sabin, S. Sugiyama, and J. A. Kindwali. 1925. The role of the monocyte in tuberculosis. *Bull. Johns Hopkins Hosp.* 37: 231.
12. Tailleux, L., O. Schwartz, J. L. Herrmann, E. Pivert, M. Jackson, A. Amara, L. Legres, D. Dreher, L. P. Nicod, J. C. Gluckman, et al. 2003. DC-SIGN is the major *Mycobacterium tuberculosis* receptor on human dendritic cells. *J. Exp. Med.* 197: 121–127.
13. Humphreys, I. R., G. R. Stewart, D. J. Turner, J. Patel, D. Karamanou, R. J. Snelgrove, and D. B. Young. 2006. A role for dendritic cells in the dissemination of mycobacterial infection. *Microbes Infect.* 8: 1339–1346.
14. Tian, T., J. Woodworth, M. Skold, and S. M. Behar. 2005. In vivo depletion of $CD11c^+$ cells delays the $CD4^+$ T cell response to *Mycobacterium tuberculosis* and exacerbates the outcome of infection. *J. Immunol.* 175: 3268–3272.
15. Gonzalez-Juarrero, M., T. S. Shim, A. Kipnis, A. P. Junqueira-Kipnis, and I. M. Orme. 2003. Dynamics of macrophage cell populations during murine pulmonary tuberculosis. *J. Immunol.* 171: 3128–3135.
16. Jakubzick, C., F. Tacke, J. Llodra, N. van Rooijen, and G. J. Randolph. 2006. Modulation of dendritic cell trafficking to and from the airways. *J. Immunol.* 176: 3578–3584.
17. Landsman, L., C. Varol, and S. Jung. 2007. Distinct differentiation potential of blood monocyte subsets in the lung. *J. Immunol.* 178: 2000–2007.
18. Henri, S., D. Vremec, A. Kamath, J. Waithman, S. Williams, C. Benoist, K. Burnham, S. Saeland, E. Handman, and K. Shortman. 2001. The dendritic cell populations of mouse lymph nodes. *J. Immunol.* 167: 741–748.
19. Vremec, D., and K. Shortman. 1997. Dendritic cell subtypes in mouse lymphoid organs: cross-correlation of surface markers, changes with incubation, and differences among thymus, spleen, and lymph nodes. *J. Immunol.* 159: 565–573.
20. Medeiros, M. A., O. A. Dellagostin, G. R. Armoa, W. M. Degrave, L. De Mendonca-Lima, M. Q. Lopes, J. F. Costa, J. McFadden, and D. McIntosh. 2002. Comparative evaluation of *Mycobacterium vaccae* as a surrogate cloning host for use in the study of mycobacterial genetics. *Microbiology* 148: 1999–2009.
21. Tamura, T., H. Ariga, T. Kinashi, S. Uehara, T. Kikuchi, M. Nakada, T. Tokunaga, W. Xu, A. Kariyone, T. Saito, et al. 2004. The role of antigenic peptide in $CD4^+$ T helper phenotype development in a T cell receptor transgenic model. *Int. Immunol.* 16: 1691–1699.
22. Nakano, H., and M. D. Gunn. 2001. Gene duplications at the chemokine locus on mouse chromosome 4: multiple strain-specific haplotypes and the deletion of secondary lymphoid-organ chemokine and EBI-1 ligand chemokine genes in the plt mutation. *J. Immunol.* 166: 361–369.
23. Buettner, M., C. Meinken, M. Bastian, R. Bhat, E. Stossel, G. Faller, G. Cianciolo, J. Ficker, M. Wagner, M. Rollinghoff, and S. Stenger. 2005. Inverse correlation of maturity and antibacterial activity in human dendritic cells. *J. Immunol.* 174: 4203–4209.
24. Hertz, C. J., S. M. Kiertscher, P. J. Godowski, D. A. Bouis, M. V. Norgard, M. D. Roth, and R. L. Modlin. 2001. Microbial lipopeptides stimulate dendritic cell maturation via Toll-like receptor 2. *J. Immunol.* 166: 2444–2450.
25. Somoskovi, A., G. Zissel, M. W. Ziegenhagen, M. Schlaak, and J. Muller-Quernheim. 2000. Accessory function and costimulatory molecule expression of alveolar macrophages in patients with pulmonary tuberculosis. *Immunobiology* 201: 450–460.
26. Bonecini-Almeida, M. G., S. Chitale, I. Boutsikakis, J. Geng, H. Doo, S. He, and J. L. Ho. 1998. Induction of in vitro human macrophage anti-*Mycobacterium tuberculosis* activity: requirement for IFN-γ and primed lymphocytes. *J. Immunol.* 160: 4490–4499.
27. Cowley, S. C., and K. L. Elkins. 2003. $CD4^+$ T cells mediate IFN-γ-independent control of *Mycobacterium tuberculosis* infection both in vitro and in vivo. *J. Immunol.* 171: 4689–4699.
28. Silver, R. F., Q. Li, W. H. Boom, and J. J. Ellner. 1998. Lymphocyte-dependent inhibition of growth of virulent Mycobacterium tuberculosis H37Rv within human monocytes: requirement for $CD4^+$ T cells in purified protein derivative-positive, but not in purified protein derivative-negative subjects. *J. Immunol.* 160: 2408–2417.
29. Jiao, X., R. Lo-Man, P. Guermonprez, L. Fiette, E. Deriaud, S. Burgaud, B. Gicquel, N. Winter, and C. Leclerc. 2002. Dendritic cells are host cells for mycobacteria in vivo that trigger innate and acquired immunity. *J. Immunol.* 168: 1294–1301.
30. Legge, K. L., and T. J. Braciale. 2003. Accelerated migration of respiratory dendritic cells to the regional lymph nodes is limited to the early phase of pulmonary infection. *Immunity* 18: 265–277.
31. Peters, W., J. G. Cyster, M. Mack, D. Schlondorff, A. J. Wolf, J. D. Ernst, and I. F. Charo. 2004. CCR2-dependent trafficking of F4/80dim macrophages and CD11cdim/intermediate dendritic cells is crucial for T cell recruitment to lungs infected with *Mycobacterium tuberculosis*. *J. Immunol.* 172: 7647–7653.
32. Peters, W., H. M. Scott, H. F. Chambers, J. L. Flynn, I. F. Charo, and J. D. Ernst. 2001. Chemokine receptor 2 serves an early and essential role in resistance to *Mycobacterium tuberculosis*. *Proc. Natl. Acad. Sci. USA* 98: 7958–7963.
33. Scott, H. M., and J. L. Flynn. 2002. *Mycobacterium tuberculosis* in chemokine receptor 2-deficient mice: influence of dose on disease progression. *Infect. Immun.* 70: 5946–5954.
34. Iezzi, G., A. Frohlich, B. Ernst, F. Ampenberger, S. Saeland, N. Glaichenhaus, and M. Kopf. 2006. Lymph node resident rather than skin-derived dendritic cells initiate specific T cell responses after *Leishmania major* infection. *J. Immunol.* 177: 1250–1256.
35. Hanekom, W. A., M. Mendillo, C. Manca, P. A. Haslett, M. R. Siddiqui, C. Barry, III, and G. Kaplan. 2003. *Mycobacterium tuberculosis* inhibits maturation of human monocyte-derived dendritic cells in vitro. *J. Infect. Dis.* 188: 257–266.

Instruction of naive CD4$^+$ T-cell fate to T-bet expression and T helper 1 development: roles of T-cell receptor-mediated signals

Haruyuki Ariga,[1,2]* Yoko Shimohakamada,[1]* Makiyo Nakada,[1,3] Takeshi Tokunaga,[1] Takeshi Kikuchi,[1,4] Ai Kariyone,[1] Toshiki Tamura[1]† and Kiyoshi Takatsu[1]

[1]*Division of Immunology, Department of Microbiology and Immunology, Institute of Medical Science, University of Tokyo, Tokyo, Japan,* [2]*First Department of Internal Medicine, Kyorin University School of Medicine, Tokyo, Japan,* [3]*Department of Pediatrics, Tokyo Women's Medical University Medical Center East, Tokyo, Japan and* [4]*Department of Pediatric Surgery, Nihon University School of Medicine, Tokyo, Japan*

doi:10.1111/j.1365-2567.2007.02630.x
Received 8 December 2006; revised 19 March 2007; accepted 26 March 2007.
*These authors contributed equally to this work.
†Present address: Department of Microbiology, Leprosy Research Center, National Institute of Infectious Disease, Tokyo, Japan.
Correspondence: Drs K. Takatsu and T. Tamura, Division of Immunology, Department of Microbiology and Immunology, Institute of Medical Science, University of Tokyo, 4-6-1 Shirokanedai, Minato-Ku, Tokyo 108–8639, Japan.
Email: takatsuk@ims.u-tokyo.ac.jp (K. Takatsu) and toshikit@ims.u-tokyo.ac.jp (T. Tamura)
Senior authors: Haruyuki Ariga, email: arigah-in@tokyo-hosp.jp and Yoko Shimohakamada, email: ssdd@ims.u-tokyo.ac.jp

Summary

Using T-cell receptor (TCR) transgenic mice, we demonstrate that TCR stimulation of naive CD4$^+$ T cells induces transient T-bet expression, interleukin (IL)-12 receptor β2 up-regulation, and GATA-3 down-regulation, which leads to T helper (Th)1 differentiation even when the cells are stimulated with peptide-loaded I-A^b-transfected Chinese hamster ovary cells in the absence of interferon-γ (IFN-γ) and IL-12. Sustained IFN-γ and IL-12 stimulation augments naive T-cell differentiation into Th1 cells. Intriguingly, a significant Th1 response is observed even when T-bet$^{-/-}$ naive CD4$^+$ T cells are stimulated through TCR in the absence of IFN-γ or IL-12. Stimulation of naive CD4$^+$ T cells in the absence of IFN-γ or IL-12 with altered peptide ligand, whose avidity to the TCR is lower than that of original peptide, fails to up-regulate transient T-bet expression, sustains GATA-3 expression, and induces differentiation into Th2 cells. These results support the notion that direct interaction between TCR and peptide-loaded antigen-presenting cells, even in the absence of T-bet expression and costimulatory signals, primarily determine the fate of naive CD4$^+$ T cells to Th1 cells.

Keywords: helper T cells (Th cells, Th0, Th1, Th2, Th3); MHC–peptide interactions; T-cell receptor (TCR); transcription factors/gene regulation

Introduction

The helper T cell is responsible for orchestrating an appropriate immune response against a wide variety of pathogens. Naive CD4$^+$ T cells recognize antigenic peptide in context of class II major histocompatibility complex (MHC) molecules on antigen-presenting cells (APCs), and subsequently differentiate into effector T

Abbreviations: TCR, T-cell receptor; IL, interleukin; Th, T helper; IFN, interferon; MHC, major histocompatibility complex; APCs, antigen-presenting cells; TNF, tumour necrosis factor; STAT, signal transducer and activator of transcription; R, receptor; P25 TCR-Tg mice, TCR transgenic mice that recognize Peptide-25; APL, altered peptide ligand; FITC, fluorescein isothiocyanate; PE, phycoerythrin; L, ligand; WT, wild type; I-A^b-CHO, Chinese hamster ovary cells expressing I-A^b; FACS, fluorescence-activated cell sorting; CFSE, 5-carboxyfluorescein diacetate succinimidyl ester; PCR, polymerase chain reaction.

© 2007 The Authors Journal compilation © 2007 Blackwell Publishing Ltd,

helper (Th) cells. $CD4^+$ Th cells are classified into two subsets of Th cells, Th1 and Th2.[1,2] Th1 cells secrete interferon-γ (IFN-γ), interleukin (IL)-2, tumour necrosis factor-α (TNF-α), and TNF-β, and are responsible for cell-mediated immunity and the eradication of intracellular pathogens. Th1 cells are also involved in transplant rejection, and protection from neoplasms.[3] Th2 cells produce IL-4, IL-5 and IL-13, these cytokines are crucial for optimal antibody production, and are essential for the effective elimination of extracellular organisms, such as helminths and nematodes.[3] Excessive production of Th1-type cytokines has been associated with the tissue destruction found in various autoimmune diseases, whereas over production of Th2-type cytokines have been implicated in atopy and allergic asthma. Therefore, elucidation of the mechanisms involved in the activation of naive $CD4^+$ T cells and differentiation of the T cells into each Th subset is of central importance in understanding immune regulation. Our knowledge of Th cell biology has increased substantially over the past two decades[4] but the molecular mechanisms regulating the initiation of either a Th1 or Th2 response remain incompletely understood.

The $CD4^+$ T-cell differentiation process is initiated when the T-cell receptor (TCR) on a naive Th cell encounters its cognate antigen, which is bound to MHC class II molecules on APC. The stimulus delivered via the TCR, in conjunction with activation of costimulatory pathways, is essential for the progression of Th cell differentiation. Upon TCR engagement a number of factors influence the differentiation process toward the Th1 or Th2 lineage, including the type of APC, the concentration of antigen (duration and strength of signal), the ligation of costimulatory molecules, and the local cytokine environment.[5–7] The most clearly defined factors determining Th subset differentiation from naive $CD4^+$ T cells are cytokines such as IL-4 and IL-12 present at the initiation of the immune response both during and after the TCR ligation. Using mice deficient for signal transducer and activator of transcription (STAT), it has been shown that activation of the IL-12 receptor (R)/STAT4 signalling pathway is important for the differentiation of naive $CD4^+$ T cells into Th1 subset.[8,9] In contrast, the IL-4R/STAT6 signalling pathway plays a central role in the differentiation of naive $CD4^+$ T cells into Th2 subset.[10–12] Determination of Th cell differentiation is also regulated by changes in the chromatin structure surrounding the Th cytokine genes, *ifn-γ* and *il-4/il-13*.[13]

The activation of naive $CD4^+$ T cells requires two separate signals. The TCR/CD3 complex delivers the first signal after its interaction with MHC peptide complex on APC. Several studies claim that the potency of TCR signalling regulates the differentiation of naive $CD4^+$ T cells into Th1 and Th2 subsets. Stimulation with high affinity peptides and high antigen dose favours Th1 differentiation and stimulation with low affinity peptides and low antigen dose favours Th2 differentiation.[14–16] However, it is still controversial whether TCR signals play a critical role in the fate of Th cell differentiation. The second signal is costimulatory, and acts through several accessory molecules on the APC that interact with their ligands on T cells such as CD28-CD80/CD86, CD152 (cytolytic T lymphocyte-associated antigen-4)–CD80/CD86, CD134 (OX40)–CD252 (OX40 ligand), CD278 (inducible costimulator)–CD275 (B7h), and CD11a (leucocyte function-associated antigen-1 (LFA-1))–CD54 (intracellular adhesion molecule-1).[17–23]

A critical stage in the differentiation process naive to Th1 $CD4^+$ T cells occurs with the induction of a transcription factor, T-bet.[24,25] T-bet is a 'master regulator' of Th1 differentiation through the up-regulation of IFN-γ and suppression of Th2-associated cytokine expression. In $CD4^+$ T cells, T-bet is rapidly and specifically induced in developing Th1 cells but not Th2 cells. T-bet expression appears to be controlled by both the TCR and the IFN-γR/STAT1 signal transduction pathways.[26,27] A regulatory circuit involving IFN-γR signalling maintains, via STAT1, a high-level T-bet expression in developing Th1 cells.[26,27] Thus, T-bet mediates STAT1-dependent processes involved in Th1 development. T-bet also induces IL-12Rβ2 expression[27,28] allowing IL-12/STAT4 signalling to optimize IFN-γ production, thereby completing the Th1 developmental commitment process. From these studies it is still unclear whether TCR signals enable T-bet to specify commitment towards Th1, IL-12Rβ2 expression and primary IFN-γ production, or whether TCR signals act to stabilize pre-existing Th1/Th2 commitment decisions.

Ag85B elicits a strong Th1 response *in vitro* in T cells both from purified protein derivatives-positive asymptomatic human subjects and Ag85B-primed cells of C57BL/6 ($I\text{-}A^b$) mice. Peptide-25 (aa240–254 FQDAYNAAGGH NAVF) of Ag85B is a major epitope recognized by Th1 cells. Active immunization of C57BL/6 mice with Peptide-25 induces the differentiation of $CD4^+$ TCR $V\beta11^+$ T cells into Th1 cells.[29–32] To elucidate molecular mechanisms of Th1 differentiation and examine the role of TCR signalling on T-bet expression, we analysed T-bet expression in naive $CD4^+$ T cells of TCR transgenic mice (P25 TCR-Tg) that recognize Peptide-25 in conjunction with $I\text{-}A^b$. Here we present evidence that indicates that direct interaction between TCR and Peptide-25-loaded APC directly determines the differentiation of naive $CD4^+$ T cells towards the Th1 subset without T-bet expression, cytokine costimulation or surface bound molecular costimulation.

Materials and methods

Mice

P25 TCR-Tg mice were generated as previously described.[33] C57BL/6 mice were purchased from the Japan SLC Inc. (Hamamatsu, Japan). $RAG\text{-}2^{-/-}$ mice were purchased from Jackson Laboratory (Bar Harbor, ME) and backcrossed five

© 2007 The Authors Journal compilation © 2007 Blackwell Publishing Ltd, *Immunology*

times with C57BL/6 mice. IFN-$\gamma^{-/-}$ mice (C57BL/6 background) were kindly provided by Dr Y. Iwakura (University of Tokyo, Tokyo, Japan). T-bet$^{-/-}$ mice[34] were kindly provided by Dr L. H. Glimcher (Harvard School of Public Health, Boston, MA), and were backcrossed with C57BL/6 mice more than six generations. IL-12/IL-18$^{-/-}$ mice[35] (C57BL/6 background) were kindly provided by Dr K. Nakanishi (Hyogo College of Medicine, Nishinomiya, Japan). STAT1$^{-/-}$ mice (C57BL/6 Background) were kindly provided by Dr R. D. Schreiber (Washington University School of Medicine, St. Louis, MO). P25 TCR-Tg mice were bred to RAG-2$^{-/-}$, IFN-$\gamma^{-/-}$, STAT1$^{-/-}$ or T-bet$^{-/-}$ mice. All mice were maintained under specific pathogen-free conditions in our animal facility according to our Institute's guideline, and used at 8–15 weeks of age.

Reagents and antibodies

Peptide-25 (FQDAYNAAGGHNAVF), and altered peptide ligand (APL) (G248A: FQDAYNAAAGHNAVF) were synthesized by Funakoshi Co. Ltd. (Tokyo, Japan). Contamination of lipopolysaccharide in peptide preparations was undetectable (<0·05 EU/ml), assessed by Endosafe^{R}-PTS (Japanese Charles River Co. Ltd, Tokyo, Japan). Anti-IFN-γ–fluorescein isothiocyanate (FITC; XMG1.2), anti-IL-4-allophycocyanin (11B11), anti-Vβ11–phycoerythrin (PE; RR3-15), anti-CD3ε–FITC (145-2C11), anti-CD4–FITC or –PE(GK1.5), anti-CD25–FITC (7D4), anti-CD28–FITC (37.51), anti-CD44–PE (IM7), anti-CD62 ligand (L)–FITC (MEL-14), anti-CD69–FITC (H1.2F3) and anti-LFA−1-FITC (2D7) were purchased from BD Bioscience PharMingen (San Diego, CA). Purified anti-CD3ε, anti-IFN-γ (R4-6A2) and anti-IL-12 (C17.8) were purchased from BD Bioscience PharMingen. IL-4 was purchased from R & D Systems (Minneapolis, MN).

Preparation of naive CD4$^+$ T cells and APC

Splenic CD4$^+$ T cells from P25 TCR-Tg or wild type (WT) C57BL/6 mice were enriched by using BD^{TM} IMag mouse CD4 T lymphocyte enrichment system (BD Bioscience PharMingen) according to the manufacturer's instructions. CD44^{low} CD62L^{high} CD4$^+$ T cells were purified from splenic CD4$^+$ T cells by sorting with FACSAria (Becton Dickinson, Mountain View, CA) after staining with anti-CD44–PE and anti-CD62L–FITC and were used as naive CD4$^+$ T cells. The purity of naive cells was >99%.

Splenocytes from WT or IL-12/IL-18$^{-/-}$ mice were labelled with a mixture of biotin anti-Thy1.2, biotin anti-DX5 and streptavidin particle-DM (BD Bioscience PharMingen) to deplete T cells and natural killer (NK) cells. Cells were then recovered by magnetic separation. Recovered cells were irradiated with a total of 3500 rad, and used as APCs. Chinese hamster ovary cells expressing I-A^b (I-A^b-CHO) (kindly provided by Dr Y. Fukui, Kyushu University, Fukuoka, Japan) were incubated with peptides for 12 hr, extensively washed and incubated with 50 μg/ml of mitomycin C for 15 min at 37° and used as APCs.

In vitro *culture of CD4$^+$ T cells*

For cell culture throughout the present experiments, complete medium consisting of RPMI-1640 with 8% fetal calf serum (Sigma-Aldrich Co., St. Louis, MO), 50 μM 2-mercaptoethanol, 50 IU/ml of penicillin and 50 μg/ml of streptomycin was used.

To examine Th differentiation *in vitro*, two-step cultures were employed. For the first culture, purified naive CD4$^+$ T cells (5×10^5 cells/ml) were activated for 6 days with peptides in the presence of T cell- and NK cell-depleted APC ($2{\cdot}5 \times 10^6$ cell/ml) or with peptide-loaded I-A^b-CHO cells ($2{\cdot}5 \times 10^5$ cells/ml) in a 48-well plate. IL-12 (10 ng/ml) and anti-IL-4 (10 μg/ml) were added to the culture to create Th1-skewing conditions, IL-4 (5 ng/ml), anti-IFN-γ (10 μg/ml) and anti-IL-12 (10 μg/ml) were added to create Th2-skewing conditions, or there was no addition of exogenous cytokines or antibodies, hereafter referred to as non-skewing conditions. In some experiments, purified naive CD4$^+$ T cells were stimulated with 10 μg/ml of soluble anti-CD3 in the presence of T cell- and NK-cell depleted APC. For the second culture, the cells collected from the first culture were washed, and the viable primed CD4$^+$ T cells were re-stimulated with 1 μg/well of plate-coated anti-CD3.

Intracellular cytokine staining and fluorescence-activated cell sorting (FACS) analysis

Cytokine-producing cells were identified by cytoplasmic staining with anti-cytokine antibodies as previously described.[36] Briefly, the stimulated cells were stained for Vβ11 or CD4, fixed, permeabilized and stained for IFN-γ and IL-4. The cells stained were gated on live Vβ11- or CD4-positive cells and analysed on a FACSCalibur (Becton Dickinson). The percentages of IL-4- and IFN-γ-producing cells are presented in the upper left and the lower right regions of Figs 1–3, 5, respectively.

To examine expression of cell surface molecules on naive CD4$^+$ T cells, purified CD4$^+$ T cells were stained with antibodies against CD3, CD4, CD25, CD28, CD69, or LFA-1. The cells stained were gated on live cells and analysed on a FACSCalibur.

Proliferation assay

Division cycle number of CD4$^+$ T cells was determined according to procedures previously described.[37] Purified naive CD4$^+$ T cells from P25 TCR-Tg mice were suspended in RPMI-1640 at 1×10^7 cells/ml and incubated with 5 μM of 5-carboxyfluorescein diacetate succinimidyl ester (CFSE;

© 2007 The Authors Journal compilation © 2007 Blackwell Publishing Ltd,

Molecular Probes, Eugene, OR) at room temperature for 15 min. The labelled $CD4^+$ T cells were washed with culture medium and then cultured with peptide in the presence of T cell- and NK cell-depleted APC for various periods of time. After the culture, the cells recovered were stained for CD4 and Vβ11, and then suspended in phosphate-buffered saline containing 2% fetal calf serum, 0·05% sodium azide and 2 μg/ml 7-amino-actinomycin D (Sigma-Aldrich Co.) to exclude dead cells from the analysis. Analyses of cell division cycle number among viable cells were conducted using FACSCalibur.

Quantitative fluorogenic real-time polymerase chain reaction (PCR)

For quantitative fluorogenic PCR experiments, real-time LightCycler PCR system (Roche Diagnostics, Basel, Switzerland) with FastStart Master Hybridization Probe (Roche Diagnostics) was used. After extracting RNA from primary or secondary stimulated cells with RNeasy (QIAGEN Inc. Valencia, CA), cDNA was reverse transcribed with 0·5 μg of Oligo(dT)12–18 and Superscript III (Invitrogen Co., Carlsbad, CA) following the instructions of the manufacturer. Primers and probes were hypoxanthine phosphoribosyl-transferase (HPRT) sense primer, 5′-GTT AAG CAG TAC AGC CCC AA-3′, HPRT antisense primer, 5′-TCA AGG GCA TAT CCA ACA AC-3′, HPRT probes, 5′-TCC AAC AAA GTC TGG CCT GTA TCC AA-FITC-3′, 5′-LC Red640-ACT TCG AGA GGT CCT TTT CAC CAG CA-3′; IL-12Rβ2 sense primer, 5′-GGC ATT TAC TCT CCT GTC-3′, IL-12Rβ2 antisense primer, 5′-GAG ATT ATC CGT AGG TAG C-3′ IL-12Rβ2 probes, 5′-CAA TGG TAT AGC AGA ACC ATT CCA GAT C-FITC-3′, 5′-LC Red640-AGC AAA CAG CAC TTG GGT AAA GAA GTA TC-3′; T-bet sense primer, 5′-CCT CTT CTA TCC AAC CAG TAT C-3′, T-bet antisense primer, 5′-CTC CGC TTC ATA ACT GTG T-3′, T-bet probes, 5′-CAT ATC CTT GGG CTG GCC TGG AAG-FITC-3′, 5′-LC Red640-TCG GGG TAG AAA CGG CTG GGA A-3′; GATA-3 sense primer, 5′-GAA GGC ATC CAG ACC CGA AAC-3′, GATA-3 antisense primer, 5-ACC CAT GGC GGT GAC CAT GC-3′, GATA-3 probes, 5′-AGC TGC TCT TGG GGA AGT CCT-FITC-3′, 5′-LC Red640-CAG CGC GTC ATG CAC CTT T-3′.

Results

Th1 differentiation of P25 TCR-Tg $CD4^+$ T cells can be induced in an IFN-γ- and IL-12-independent manner

P25 TCR-Tg mice, that expressed TCR-α5 and -β11 chains on $CD4^+$ T cells in peripheral blood, the spleen, lymph node and thymocytes, were generated. FACS analysis revealed that over 98% of splenic $CD4^+$ T cells from RAG-$2^{-/-}$ P25 TCR-Tg mice expressed TCR Vβ11-chain. T-bet and IFN-γ mRNA expression was not detected, by RT-PCR, in splenic $CD4^+$ cells of RAG-$2^{-/-}$ P25 TCR-Tg mice (data not shown), suggesting that $CD4^+$ T cells in P25 TCR-Tg mice are not preactivated.

RAG-$2^{-/-}$ P25 TCR-Tg naive $CD4^+$ splenic T cells were stimulated *in vitro* for 6 days with Peptide-25 in the presence of APC. After 6 days in culture, the proliferated cells were harvested and re-stimulated for another day with plate-coated anti-CD3. After culturing, IFN-γ- and IL-4-producing cells were analysed by cytoplasmic staining. Naive $CD4^+$ T cells stimulated with Peptide-25 in the presence of APC became solely IFN-γ-producing cells under non-skewing conditions (Fig. 1a, left hand panel). When RAG-$2^{-/-}$ P25 TCR-Tg naive $CD4^+$ T cells were cultured with Peptide-25 in the presence of APC, IL-4, anti-IFN-γ and anti-IL-12 (Th2-skewing conditions), a significant proportion of the T cells became IL-4-producing cells (Fig. 1a, right hand panel), while IFN-γ-producing T cells were undetectable. These results indicate that Peptide-25 TCR-Tg naive $CD4^+$ T cells are not precommitted to differentiation towards Th1 before P25 stimulation and retain the potential to differentiate into both Th1 and Th2 lineages.

In addition to the TCR signals IFN-γ and IL-12 play an important role in Th1 development and differentiation. Naive $CD4^+$ T cells from RAG-$2^{-/-}$ P25 TCR-Tg mice were stimulated with Peptide-25 and APC in the presence of anti-IFN-γ, anti-IL-12 or a combination of them for 6 days. FACS analysis revealed that in cultures of $CD4^+$ T cells from RAG-$2^{-/-}$ P25 TCR-Tg mice (Fig. 1a), substantial numbers of IFN-γ-producing cells were observed even when stimulated in the presence of anti-IFN-γ and anti-IL-12.

To confirm bioactivities of anti-IFN-γ and anti-IL-12, we stimulated naive $CD4^+$ T cells from WT mice with anti-CD3 in the presence of splenic APC together with or without anti-IFN-γ and anti-IL-12. Addition of anti-IFN-γ and anti-IL-12 completely blocked anti-CD3-induced-Th1 differentiation (Fig. 1b). We also confirmed, in separate experiments by using bioassay and enzyme-linked immunosorbent assay, that each of the anti-cytokine antibodies could completely neutralize relevant cytokine activity specifically.

Stimulation of P25 TCR-Tg naive $CD4^+$ T cells with IL-12/IL-$18^{-/-}$ splenic APC and Peptide-25 induced differentiation into IFN-γ-producing cells. This was quantitatively similar to the differentiation seen under conditions of Peptide-25 stimulation in the presence of WT APC (Fig. 1c). These results imply that IFN-γ and IL-12 are not essential for development of Th1 cells from naive $CD4^+$ T cells in response to Peptide-25.

Commitment of P25 TCR-Tg $CD4^+$ T cells to Th1 differentiation is determined within 3 days after Peptide-25 and splenic APC stimulation

It has been shown that IFN-γ and IL-12 play important roles in sustained development and differentiation of

© 2007 The Authors Journal compilation © 2007 Blackwell Publishing Ltd, *Immunology*

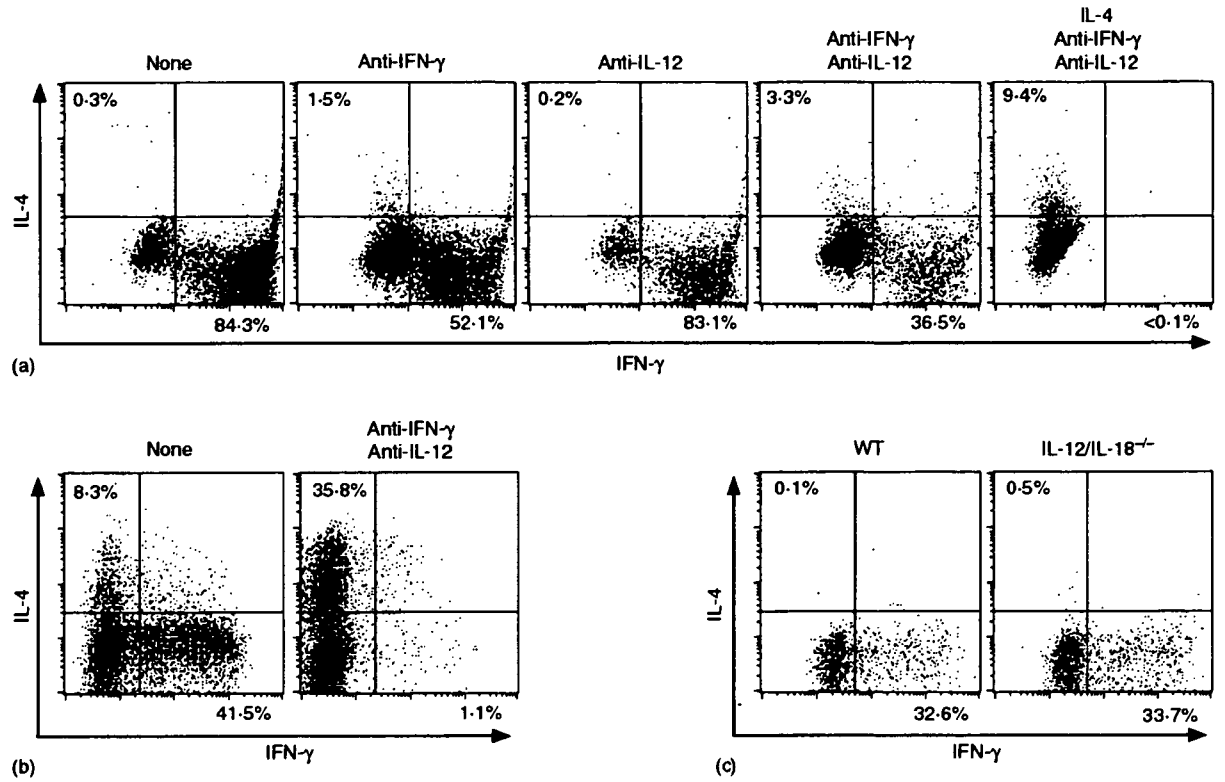

Figure 1. Th1 differentiation of P25 TCR-Tg naive $CD4^+$ T cells upon Peptide-25 stimulation is independent on IFN-γ, IL-12 and IL-18. (a) Naive $CD4^+$ T cells from RAG-$2^{-/-}$ P25 TCR-Tg mice were stimulated *in vitro* with 10 μg/ml of Peptide-25 for 6 days in the presence of splenic APC. On day 0, some groups of culture received anti-IFN-γ, anti-IL-12, IL-4 or a combination of these, as depicted in (a). After the culture the primed cells were re-stimulated and IFN-γ- and IL-4-producing cells were assessed. Events shown are gated on live $V\beta11^+$ cells. Results are presented for one of three experiments performed, with similar results in each experiment. (b) Naive $CD4^+$ T cells from WT C57BL/6 were stimulated *in vitro* with 10 μg/ml of soluble anti-CD3 in the presence of splenic APC. On day 0, a group of culture received anti-IFN-γ and anti-IL12. After the culture the primed cells were re-stimulated and IFN-γ- and IL-4-producing cells were assessed. Events shown are gated on live $CD4^+$ cells. Representative results of two separate experiments were displayed. (c) P25 TCR-Tg naive $CD4^+$ T cells were stimulated *in vitro* with 10 μg/ml of Peptide-25 in the presence of splenic APC from WT or IL-12/IL-$18^{-/-}$ mice. After the culture the primed cells were re-stimulated and IFN-γ- and IL-4-producing cells were assessed. Events shown are gated on live $V\beta11^+$ cells. Representative results of two separate experiments were displayed.

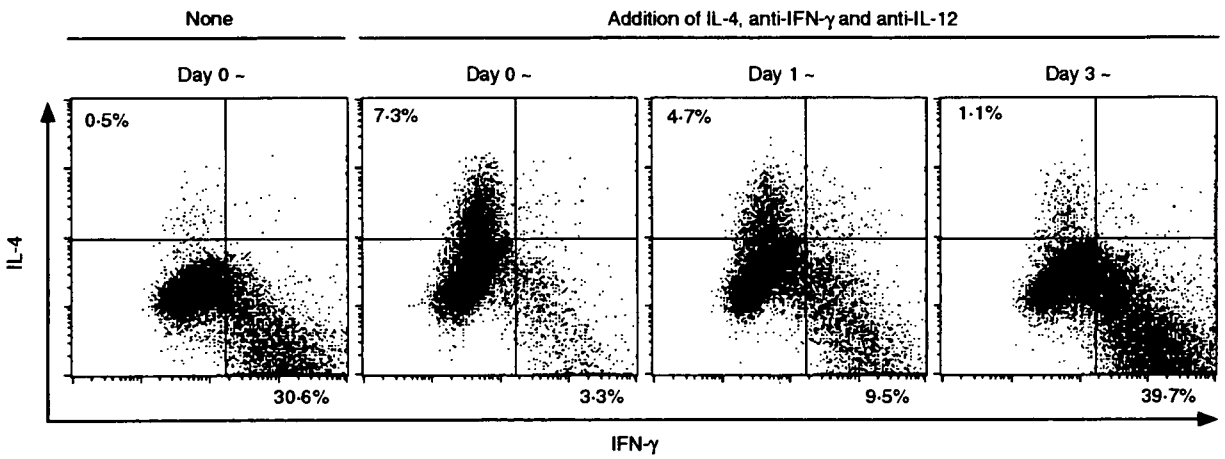

Figure 2. Commitment to Th1 differentiation of P25 TCR-Tg $CD4^+$ T cells occurs within 3 days after stimulation with Peptide-25. P25 TCR-Tg naive $CD4^+$ T cells were separated into four groups. Each group was stimulated with 10 μg/ml of Peptide-25 in the presence of splenic APC. IL-4, anti-IFN-γ and anti-IL-12 were added into each of three groups of culture on days 0, 1, and 3. After the culture the primed cells were re-stimulated and IFN-γ- and IL-4-producing cells were assessed. Events shown are gated on live $V\beta11^+$ cells. Representative results of three separate experiments were displayed.

© 2007 The Authors Journal compilation © 2007 Blackwell Publishing Ltd, *Immunology*

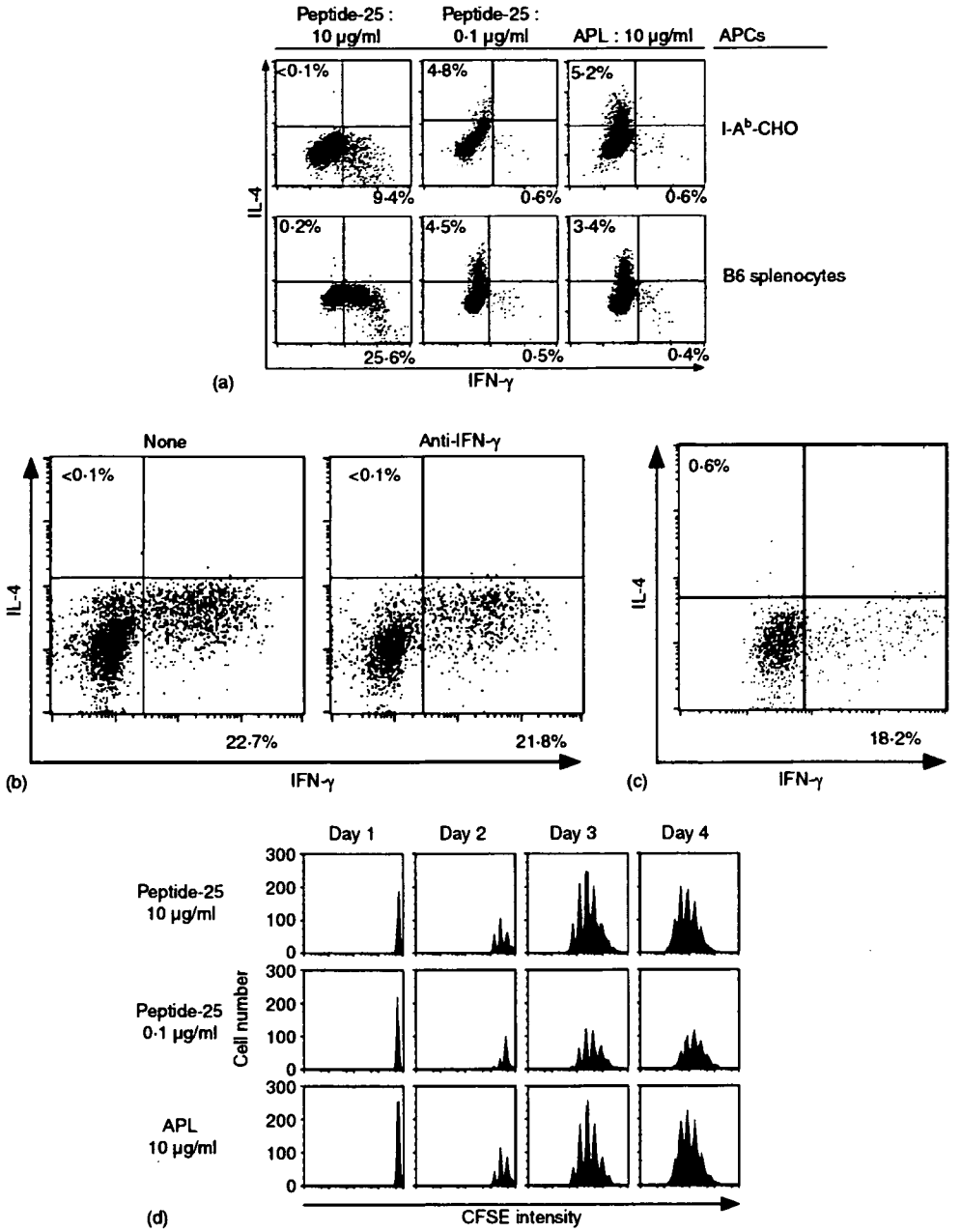

Figure 3. Th1 differentiation of P25 TCR-Tg naive CD4$^+$ T cells can be induced in Peptide-25-loaded antigen-presenting cells lacking nominal costimulatory molecules. (a) P25 TCR-Tg naive CD4$^+$ T cells were stimulated *in vitro* with 10 μg/ml or 0·1 μg/ml of Peptide-25 or 10 μg/ml of APL in the presence of I-A^b-CHO or splenic APC. After the culture the primed cells were re-stimulated and IFN-γ- and IL-4-producing cells were assessed. Events shown are gated on live Vβ11$^+$ cells. Representative results of three separate experiments were displayed. (b) Naive CD4$^+$ T cells from P25 TCR-Tg were stimulated *in vitro* with Peptide-25-loaded I-A^b-CHO in the presence or absence of anti-IFN-γ. After the culture the primed cells were re-stimulated and IFN-γ- and IL-4-producing cells were assessed. Events shown are gated on live Vβ11$^+$ cells. Results are presented for one of three experiments performed, with similar results in each experiment. (c) Naive CD4$^+$ T cells from STAT1$^{-/-}$ P25 TCR-Tg mice were stimulated *in vitro* with Peptide-25-loaded I-A^b-CHO. After the culture the primed cells were re-stimulated and IFN-γ- and IL-4-producing cells were assessed. Events shown are gated on live Vβ11$^+$ cells. Results are presented for one of three experiments performed, with similar results in each experiment. (d) Naive CD4$^+$ T cells from P25 TCR-Tg mice were labeled with 5 μM of CFSE and stimulated with 10 μg/ml or 0·1 μg/ml of Peptide-25 or 10 μg/ml of APL in the presence of splenic APC. On the days indicated, CD4$^+$ T cells were harvested, stained for CD4 and Vβ11, and then analysed for dilution of CFSE intensity by FACSCalibur. Events shown are gated on live CD4^{+-} Vβ11$^+$ cells.

Th1 cells. To examine the roles of IFN-γ and IL-12 in the stabilization of Th1 differentiation, we established four groups of P25 TCR-Tg naive CD4$^+$ T cells, cultured for 6 days in the presence of Peptide-25 and APC. During the culture periods, three groups of culture received a mixture of IL-4, anti-IFN-γ and

© 2007 The Authors Journal compilation © 2007 Blackwell Publishing Ltd, *Immunology*

anti-IL-12 on day 0, 1, or 3, for converting non-skewing to Th2-skewing conditions. After culturing with Peptide-25 and APC, the proportions of IFN-γ- and IL-4-producing cells were quantified. Adding IL-4, anti-IFN-γ, and anti-IL-12 on day 0 or 1 caused the proportion of cells producing IL-4 to be significantly increased, whereas the proportion of cells producing IFN-γ decreased (Fig. 2). Addition of IL-4, anti-IFN-γ and anti-IL-12 to the culture on day 3 or thereafter was ineffective and predominant proportions of IFN-γ-producing cell were observed. These results suggest that IFN-γ and IL-12 are indispensable for the full commitment of naive $CD4^+$ T cells to Th1 differentiation, and for the stabilization of Th1-developing cells within 3 days after onset of culture.

Peptide-25-stimulated $CD4^+$ T cells of P25 TCR-Tg mice are able to differentiate to Th1 cells independently of costimulatory molecules

The current dogma of Th cell differentiation is that costimulation of naive $CD4^+$ T cells via membrane-bound molecules on the APC plays an important role in determining Th differentiation into Th1 or Th2 subset. To examine the role of costimulatory molecules in Th1 development, P25 TCR-Tg naive $CD4^+$ T cells were stimulated for 6 days *in vitro* with various concentrations of Peptide-25 or APL in the presence of I-A^b-CHO, because I-A^b-CHO does not express detectable levels of CD54, CD80, CD86, CD252 and CD275. APL has weaker avidity to P25 TCR than Peptide-25 (less than 1/30).[36] As a control, splenic APC was also used. The majority of cytokine-producing T cells were IFN-γ-producing cells, when 10 μg/ml (6·0 μM) of Peptide-25 in the presence of I-A^b-CHO was used as the stimulant (Fig. 3a, upper panel). The T cells stimulated with 0·1 μg/ml (0·06 μM) of Peptide-25 or 10 μg/ml (6·0 μM) of APL in the presence of I-A^b-CHO differentiated into IL-4-producing cells. Essentially similar results were obtained when P25 TCR-Tg naive $CD4^+$ T cells were stimulated with Peptide-25 or APL in the presence of splenic APC in place of I-A^b-CHO (Fig. 3a, lower panel). Considerable proportions of IFN-γ-producing cells were detected even when anti-IFN-γ was added during the culture of naive $CD4^+$ T cells with Peptide-25 in the presence of I-A^b-CHO (Fig. 3b). Furthermore, naive $CD4^+$ T cells from $STAT1^{-/-}$ P25 TCR-Tg mice could differentiate into solely IFN-γ-producing cells when they were cultured with Peptide-25-loaded I-A^b-CHO (Fig. 3c).

There remains a possibility that our observation might be simply explained with the difference in proliferative rate between Th1 and Th2 cells. The cell recovery after culturing P25 TCR-Tg naive $CD4^+$ T cells stimulated with low dose Peptide-25 (0·1 μg/ml) that induced Th2 differentiation was approximately 65% of that stimulated with high dose Peptide-25 (10 μg/ml) that induced Th1 differentiation. On the other hand, the cell recovery after stimulation of P25 TCR-Tg naive $CD4^+$ T cells with APL (10 μg/ml) that induced Th2 differentiation was similar to that stimulation with high dose Peptide-25 (10 μg/ml). Furthermore, we examined the division cycle number of P25 TCR-Tg naive $CD4^+$ T cells on days 1–4 after the stimulation with 10 μg/ml or 0·1 μg/ml of Peptide-25 or 10 μg/ml of APL using the fluorescent dye CFSE. In all stimulation, the cells started to divide by 48 hr and stopped dividing by 96 hr after the stimulation (Fig. 3d). High-dose Peptide-25 and APL stimulation induced six to eight cell divisions. On the other hand, low-dose Peptide-25 induced five to seven cell divisions. These results suggest that the phenomenon described above might not be simply explained by the difference in proliferative rate between Th1 and Th2 cells.

Taken together, these results indicate that P25 TCR-Tg naive $CD4^+$ T cells do differentiate into Th1 cells in the absence of costimulatory molecules.

TCR stimulation induces T-bet up-regulation and GATA-3 down-regulation in an IFN-γ-independent manner

The expression of Th1 specific transcription factors is thought to induce chromatin remodelling of Th1-specific cytokine genes. P25 TCR-Tg naive $CD4^+$ T cells were stimulated *in vitro* with Peptide-25-loaded I-A^b-CHO for various periods of time. The expression of T-bet, GATA-3 and IL-12Rβ2 was analysed periodically by quantitative real-time PCR. Three hr after stimulation (early phase), T-bet expression was elevated up to 70–110-fold over unstimulated cells, by 9 hr after stimulation the expression level of T-bet sharply dropped. Moreover, anti-IFN-γ presence did not affect T-bet expression. The second-phase (late-phase) of T-bet expression began after 12 hr of stimulation and peaked (50-fold higher expression over control levels) at 15 hr after the stimulation (Fig. 4a). Addition of IL-12 in the culture slightly enhanced T-bet expression, in both early and late-phases. The late-phase T-bet expression was decreased to almost the same levels as naive $CD4^+$ T cells when anti-IFN-γ was added. In contrast, GATA-3 expression was rapidly decreased after the Peptide-25 stimulation in all conditions tested. Similar analysis was carried out using naive $CD4^+$ T cells from IFN-$\gamma^{-/-}$ P25 TCR-Tg mice. Results revealed that early phase T-bet expression in IFN-$\gamma^{-/-}$ P25 TCR-Tg naive $CD4^+$ T cells was enhanced to an extent similar to that seen in WT P25 TCR-Tg naive $CD4^+$ T cells, although no late-phase T-bet expression was seen in IFN-$\gamma^{-/-}$ P25 TCR-Tg naive $CD4^+$ T cells. GATA-3 expression was down-regulated in IFN-$\gamma^{-/-}$ P25 TCR-Tg naive $CD4^+$ T cells upon stimulation similarly to that seen in WT P25 TCR-Tg naive $CD4^+$ T cells, although a slightly slower and milder down-regulation was seen. The IL-12Rβ2

© 2007 The Authors Journal compilation © 2007 Blackwell Publishing Ltd, *Immunology*

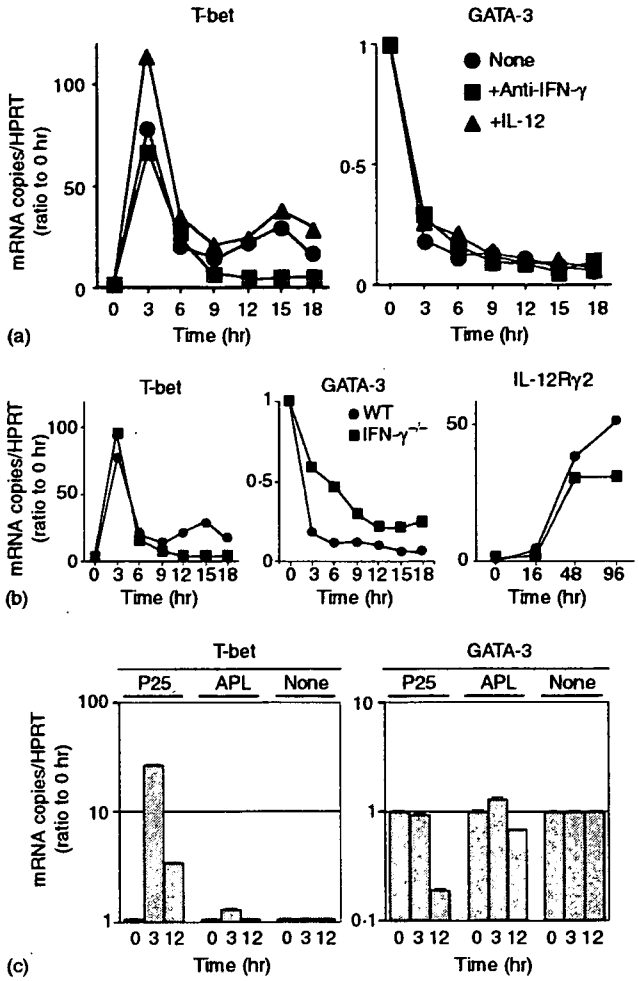

Figure 4. Kinetics of induction of T-bet, GATA-3 and IL-12Rβ2 transcripts in Peptide-25-loaded I-A^b-CHO-activated T cells. Naive CD4$^+$ T cells were stimulated for indicated periods of time (hr) with Peptide-25- or APL-loaded I-A^b-CHO. Cells were collected at the indicated time points and RNA was extracted. Quantitative real-time PCR was performed for assessing the mRNA expression of T-bet, GATA-3 or IL-12Rβ2. Each sample was normalized to HPRT. Data shown are ratios of test mRNA copies to mRNA copies of unstimulated cells. The values represent the mean and SD. When error bars are not visible they are smaller than the symbol width. Results are presented for one of three experiments performed, with similar results in each experiment. (a) P25 TCR-Tg naive CD4$^+$ T cells were stimulated with Peptide-25-loaded I-A^b-CHO alone or in the presence of anti-IFN-γ (3 μg/ml) or rIL-12 (10 ng/ml). (b) Naive CD4$^+$ T cells either from WT P25 TCR-Tg mice or IFN-γ$^{-/-}$ P25 TCR-Tg mice were stimulated with Peptide-25-loaded I-A^b-CHO. (c) P25 TCR-Tg naive CD4$^+$ T cells were stimulated with Peptide-25-loaded I-A^b-CHO or APL-loaded I-A^b-CHO. As a control, cells were incubated without any stimulus.

expression gradually increased for 48 hr after stimulation regardless of IFN-γ (Fig. 4b). Up-regulation of T-bet expression was also observed when naive CD4$^+$ T cells from STAT1$^{-/-}$ P25 TCR-Tg mice were stimulated *in vitro* with Peptide-25-loaded I-A^b-CHO in the presence of anti-IFN-γ (data not shown). These results indicate that IFN-γ/STAT1 is dispensable to induce the T-bet expression although IFN-γ/STAT1 is indispensable to maintain the expression.

We also analysed expression of T-bet and GATA-3 in P25 TCR-Tg naive CD4$^+$ T cells in response to APL-loaded I-A^b-CHO. Surprisingly, neither enhancement of T-bet expression nor down-regulation of GATA-3 was observed (Fig. 4c).

Taken together, these results suggest that the interaction between Peptide-25/I-A^b and TCR directly regulates the expression of T-bet, GATA-3, and IL-12Rβ2, thereby determining the fate of naive CD4$^+$ T cells for differentiation into Th1 subset.

Th1 differentiation can be induced in T-bet-dependent and T-bet-independent manners

We next examined the role of T-bet transcription factor in Th1 differentiation of naive CD4$^+$ T cells from P25 TCR-Tg mice by priming with Peptide-25. Expression of T-cell activation markers on naive CD4$^+$ T cells from T-bet$^{-/-}$ P25 TCR-Tg mice was comparable to these of WT P25 TCR-Tg mice (Fig. 5a). To confirm the functional deficiency of T-bet in T-bet$^{-/-}$ P25 TCR-Tg mice, we examined the IFN-γ production in primary response of naive CD4$^+$ T cells from T-bet$^{-/-}$ P25 TCR-Tg mice to anti-CD3 and anti-CD28 according to procedures previously described by Szabo *et al.*[34] Consistent with Szabo's report[34], T-bet$^{-/-}$ P25 TCR-Tg naive CD4$^+$ T cells did not produce IFN-γ, although WT P25 TCR-Tg T cells produced large amounts of IFN-γ (data not shown). These results indicate that T-bet$^{-/-}$ P25 TCR-Tg naive CD4$^+$ T cells is functionally T-bet deficient.

We compared the differentiation of naive CD4$^+$ T cells from T-bet$^{-/-}$ P25 TCR-Tg mice and naive CD4$^+$ T cells from WT P25 TCR-Tg mice in response to Peptide-25. Naive CD4$^+$ T cells from T-bet$^{-/-}$ P25 TCR-Tg mice or WT P25 TCR-Tg mice were stimulated *in vitro* for 6 days with Peptide-25 in the presence of splenic APC. After 6 days in culture, the proliferated cells were harvested and re-stimulated for another day with plate-coated anti-CD3. After culturing, IFN-γ- and IL-4-producing cells were analysed by cytoplasmic staining. Intriguingly, naive CD4$^+$ T cells from T-bet$^{-/-}$ P25 TCR-Tg mice differentiated into Th1 cells upon Peptide-25 stimulation (Fig. 5b). Naive CD4$^+$ T cells from WT P25 TCR-Tg mice, when identically stimulated, showed far higher induction of IFN-γ production. When compared between WT and T-bet null background, the lack of T-bet protein clearly reduced proportions of IFN-γ-producing Th cells from 46·5% to 14·6%, indicating that about two-third of Th1 differentiation is contributed to T-bet and one-third of the response is T-bet independent. A significant proportion became IL-4-producing T cells when naive CD4$^+$ T cells from T-bet$^{-/-}$ P25 TCR-Tg mice were stimulated

© 2007 The Authors Journal compilation © 2007 Blackwell Publishing Ltd, *Immunology*

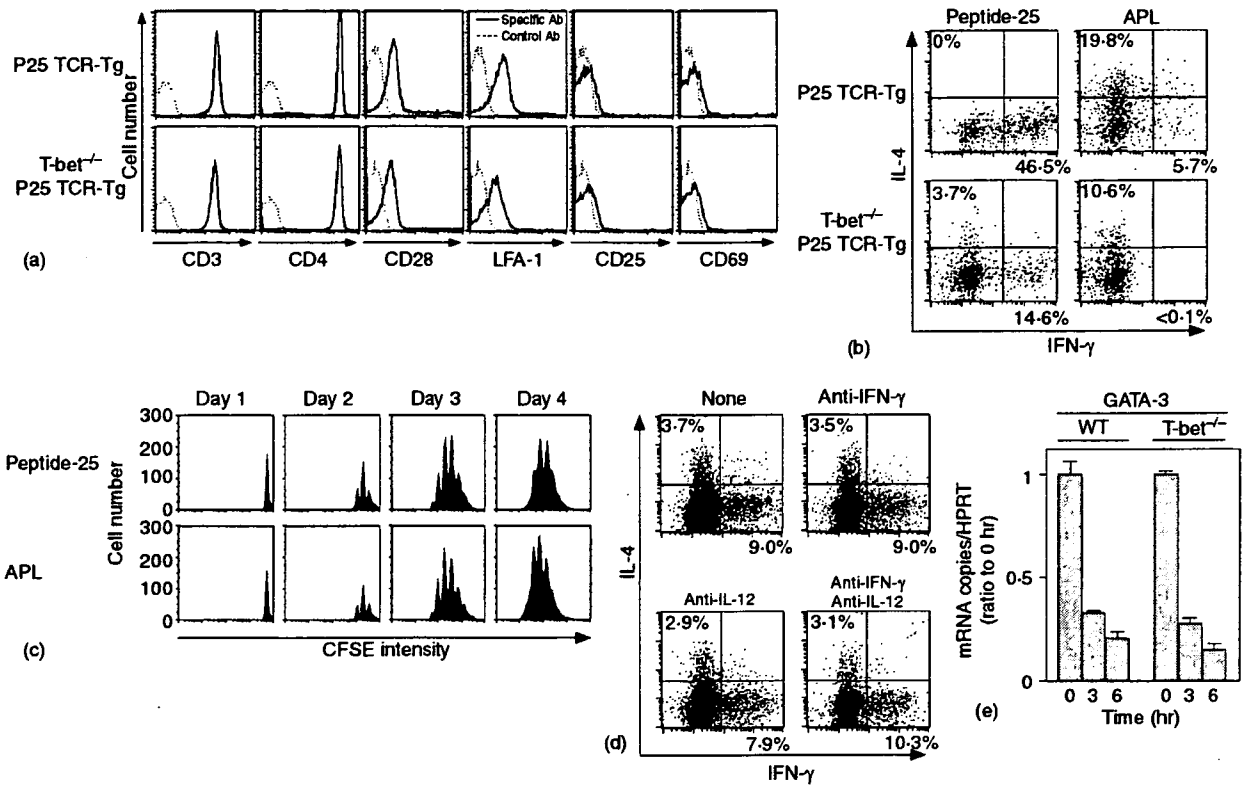

Figure 5. Induction of GATA-3 transcripts is down-regulated in Peptide-25-loaded I-A^b-CHO-stimulated T-$bet^{-/-}$ P25 TCR-Tg naive T cells. (a) Naive $CD4^+$ T cells from P25 TCR-Tg or T-$bet^{-/-}$ P25 TCR-Tg mice were stained for CD3, CD4, CD28, LFA-1, CD25 and CD69. Events shown were gated on live cells. (b) Naive $CD4^+$ T cells from P25 TCR-Tg or T-$bet^{-/-}$ P25 TCR-Tg mice were stimulated *in vitro* with 10 μg/ml of Peptide-25 in the presence of splenic APC under non-skewing conditions. After the culture the primed cells were re-stimulated and IFN-γ- and IL-4-producing cells were assessed. Events shown are gated on live $V\beta11^+$ cells. Representative results of four separate experiments were displayed. (c) Naive $CD4^+$ T cells from T-$bet^{-/-}$ P25 TCR-Tg mice were labelled with CFSE and stimulated with 10 μg/ml of Peptide-25 or 10 μg/ml of APL in the presence of splenic APC. On the days indicated, $CD4^+$ T cells were harvested, stained for CD4 and Vβ11, and analysed for dilution of CFSE intensity by FACSCalibur. Events shown are gated on live CD4 ± $V\beta11^+$ cells. (d) Naive $CD4^+$ T cells from T-$bet^{-/-}$ P25 TCR-Tg mice were stimulated with Peptide-25-loaded I-A^b-CHO. On day 0, some groups of culture received anti-IFN-γ, anti-IL-12 or a combination of these, as depicted in (d). After the culture the primed cells were re-stimulated and IFN-γ- and IL-4-producing cells were assessed. Events shown are gated on live $V\beta11^+$ cells. Results are presented for one of three experiments performed, with similar results in each experiment. (e) Naive $CD4^+$ T cells from P25 TCR-Tg or T-$bet^{-/-}$ P25 TCR-Tg mice were stimulated for indicated periods of time (hr) with Peptide-25-loaded I-A^b-CHO. Cells were collected at the indicated time points and RNA was extracted. Quantitative real-time PCR was performed for assessing the mRNA expression of GATA-3 and HPRT. Each sample was normalized to HPRT. Data shown are ratios of test mRNA copies to mRNA copies of unstimulated cells. The values represent the mean and SD. Representative results of three separate experiments were displayed.

with Peptide-25. APL stimulation predominantly induced IL-4-producing T cells (Fig. 5b). As for proliferative response, Peptide-25 and APL induced six to eight cell divisions of the T cells similarly (Fig. 5c).

To examine whether IFN-γ and IL-12 affect Th1 differentiation in T-$bet^{-/-}$ T cells, we added neutralization antibodies of IFN-γ and IL-12 to the culture of $CD4^+$ T cells from T-$bet^{-/-}$ P25 TCR-Tg mice. Results revealed that addition of anti-IFN-γ and anti-IL-12 did not alter proportions of IFN-γ- and IL-4-producing cells significantly (Fig. 5d). We infer from these results that there may be T-bet-dependent and T-bet-independent pathways for Th1 commitment and its differentiation.

Upon Peptide-25-loaded I-A^b-CHO-stimulation, GATA-3 expression in $CD4^+$ T cells of WT P25 TCR-Tg mice and T-$bet^{-/-}$ P25 TCR-Tg mice was then compared. Results revealed that Peptide-25-loaded I-A^b-CHO dependent GATA-3 expression in T-$bet^{-/-}$ P25 TCR-Tg $CD4^+$ T cells was comparable to that seen in WT P25 TCR-Tg $CD4^+$ T cells (Fig. 5e).

Discussion

The differentiation of naive $CD4^+$ T cells to either Th1 or Th2 cells is a critical aspect of any immune response, with broad implications in host defence against disease pathogenesis. Many factors influence polarization of $CD4^+$ T

© 2007 The Authors Journal compilation © 2007 Blackwell Publishing Ltd,

cells to Th1 or Th2, including those collectively termed 'strength of stimulation', such as peptide dose and duration of TCR engagement. T-cell activation requires signals emanating from the TCR complex along with those generated through costimulatory molecules, various cytokines and transcription factors, these are all key determinants of the differentiation into Th1 or Th2 cells, however, exactly what is the key primal signal is unclear.

The strength of interaction mediated through the TCR and MHC/peptide complex directly affect lineage commitment of Th cells.[16,38,39] Stimulation with high affinity peptides and high antigen dose favours Th1 differentiation and stimulation with low affinity peptides and low antigen dose favours Th2 differentiation.[14–16] The use of APL has provided convincing evidence that the strength of the signal transmitted via the TCR influences lineage commitment.[14,16] Stimulation of P25 TCR-Tg naive $CD4^+$ T cells with high dose Peptide-25 (10 μg/ml (6·0 μM)) preferentially induces Th1 development. In contrast, when T cells were stimulated with low dose Peptide-25 (0·1 μg/ml (0·06 μM)), a dominant Th2 response was observed (Fig. 3). Our observations are consistent with the published data.[15,38]

It is well known that costimulation is indispensable in Th1 and Th2 differentiation.[40] Our results showed that Th1 and Th2 differentiations could be induced when P25 TCR-Tg naive $CD4^+$ T cells were stimulated with Peptide-25-loaded and APL-loaded I-A^b-CHO, respectively (Fig. 3). As Chinese hamster ovary cells do not express detectable levels of CD54, CD80, CD86, CD252 and CD275, we are in favour of the hypothesis that preferential induction of Th1 and Th2 development upon Peptide-25 and APL stimulation, respectively, may be independent of these well-known costimulating signals from APC.

In this report, we used plate-coated anti-CD3 stimulation in second culture to evaluate the differentiation of naive $CD4^+$ T cells. It has been reported that plate-coated anti-CD3 induced the activation-induced cell death (AICD) in activated $CD4^+$ T cells[41] and Th1 cells appears to be more susceptible to AICD than Th2 cells.[42] Therefore, we compared the ability of AICD induction between plate-coated anti-CD3 and another mitogenic stimulation such as phorbol 12-myristate 13-acetate (PMA)/ionomycin. Purified naive $CD4^+$ T cells from WT C57BL/6 mice were stimulated with soluble anti-CD3 in the presence of splenic APC under either Th1- or Th2-skewing conditions for 6 days. After the culture the viable cells were restimulated with plate-coated anti-CD3 for 24 hr or 10 ng/ml of PMA and 1 μM of ionomycin for 4 hr. The AICD was assayed by FACS using 7AAD. We did not observe a significant difference in the ability of AICD induction between plate-coated anti-CD3 and PMA/ionomycin stimulations. The cells positively stained with 7AAD were 26·3% and 18·2% in Th1 cells restimulated with plate-coated anti-CD3 and PMA/ionomycin, respectively, and 25·1% and 19·8% in Th2 cells restimulated with anti-CD3 and PMA/ionomycin, respectively.

A complex network of gene transcription events is likely to be involved in establishing an environment that promotes Th1 development. It has been reported that naive $CD4^+$ T cells express little T-bet or IL-12Rβ2 and are unresponsive to IL-12, and T-bet appears to initiate Th1 lineage development from naive $CD4^+$ T cells both by activating Th1 genetic programmes and by repressing the opposing Th2 programmes.[24] It has been hypothesized that upon activation, TCR-derived signals alone may induce T-bet, but this alone is not sufficient to permit its optimal expression[26]. Interestingly, T-bet expression is markedly elevated, peaking 3 h after Peptide-25-loaded I-A^b CHO stimulation of IFN-$\gamma^{-/-}$ P25 TCR-Tg T cells (Fig. 4b) and STAT1$^{-/-}$ P25 TCR-Tg T cells as well (data not shown). Furthermore, naive $CD4^+$ T cells from STAT1$^{-/-}$ P25 TCR-Tg mice were capable of differentiating into IFN-γ-producing cells upon stimulation with Peptide-25-loaded I-A^b-CHO (Fig. 3b). IL-12Rβ2 expression detected at 24 hr after stimulation is also observed in IFN-$\gamma^{-/-}$ P25 TCR-Tg T cells. These results indicate that those T-bet and IL-12Rβ2 expressions are IFN-γ/STAT1 and costimulatory signal independent. The sustained T-bet and IL-12Rβ2 expression observed 15 h and 48 hr, respectively, after the peptide stimulation are IFN-γ/STAT1 dependent (Fig. 4b). Exposure of T cells after TCR activation to IFN-γ may be important for the sustained T-bet induction and may be relate to full Th1 differentiation. So the interaction between Peptide-25/I-A^b and P25 TCR may directly induce T-bet and IL-12Rβ2 that may lead to Th1 differentiation. Significant proportions of Peptide-25-stimulated T cells from T-bet$^{-/-}$ P25 TCR-Tg mice become IFN-γ-producing cells (Fig. 5), although large proportions of the T cells become IL-4-producing cells. Proportions of IFN-γ-producing cells in Peptide-25-stimulated T-bet$^{-/-}$ P25 TCR-Tg T cells are not altered even in the presence of anti-IFN-γ and anti-IL-12 antibodies. Therefore, IFN-γ and IL-12 are dispensable for T-bet-independent Th1 differentiation.

GATA-3 is a Th2-specific transcription factor, which is thought to be induced by STAT6 and regulate chromatin remodelling of the *Th2 cytokine* locus. It has been reported that retroviral ectopic expression of T-bet does not suppress either GATA-3 or Th2 cytokine expression in committed Th2 cells.[27] GATA-3 expression was rapidly decreased soon after the P25 TCR stimulation by Peptide-25, under the conditions tested. Activated $CD4^+$ T cells from P25 TCR-Tg mice produced IFN-γ, but not IL-4, within 24 hr of stimulation with Peptide-25-loaded I-A^b-CHO, determined by enzyme-linked immunospot assay (data not shown). These results suggest that the acute down-regulation of GATA-3 expression after stimulation with Peptide-25-loaded I-A^b-CHO may be induced

© 2007 The Authors Journal compilation © 2007 Blackwell Publishing Ltd, *Immunology*

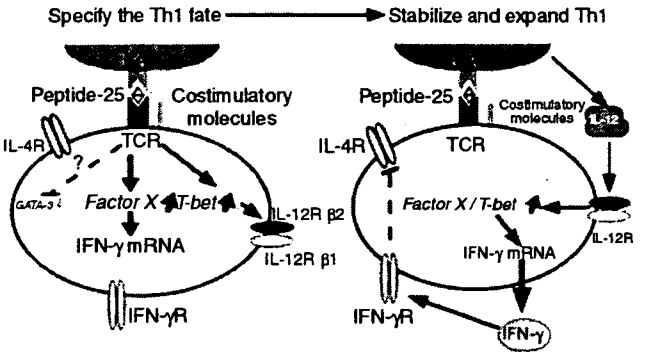

Figure 6. The pathway of Th1 development illustrates how external TCR signals play a role differently from IFN-γ and IL-12, and how these pathways are intrinsically ordered. (Left-hand panel) Antigen receptor ligation enables T-bet to specify the Th1 fate, including T-bet auto-induction, IL-12Rβ2 induction, and primary remodelling of the *ifn*-γ locus. (Right-hand panel) The actions of T-bet then enable IFN-γ and probably IL-12 to signal for survival and growth of Th1 cells, and interact for secondary enhancement of IFN-γ gene expression.

primarily as a result of TCR signals, but this may not be caused by direct inhibition through T-bet.

The results of this study have been integrated to suggest a mechanism of Th1 differentiation (Fig. 6). Immediately after TCR stimulation by Peptide-25/I-A^b, P25 TCR-Tg naive $CD4^+$ T cells express T-bet mRNA independently of IFN-γ signalling while GATA-3 expression is suppressed. This acute induction of T-bet may induce chromatin remodelling of the *ifn*-γ locus. As a result, the activated $CD4^+$ T cells transcribe IFN-γ, but not IL-4, this enhances T-bet expression further through STAT1 activation, leading to IL-12Rβ2 up-regulation and the termination of IL-4 signal transduction. IL-12 produced by activated APC maintains T-bet and IFN-γ expression through STAT4 activation. Transcription factors other than T-bet may orchestrate, with T-bet, the commitment of naive Th cells towards Th1 development.

In summary, we have presented that P25 TCR-Tg naive $CD4^+$ T cells stimulated with Peptide-25/I-A^b polarize to Th1 differentiation preferentially in the absence of IFN-γ and IL-12. Furthermore, Th1 development of naive $CD4^+$ T cells from T-$bet^{-/-}$ P25 TCR-Tg mice is inducible. We propose that direct interaction of the specific antigenic peptide MHC class II complex and TCR may primarily influence the determination of naive $CD4^+$ T cell fate in development towards the Th1 subset. The regulatory effect seems to occur independently of costimulation and Th1 inducible cytokine, IFN-γ and IL-12, and controls the fate of naive $CD4^+$ T cells for differentiation into Th1 subsets.

Acknowledgements

We thank Dr S. Takaki and all lab members for their valuable suggestions and encouragement throughout this study. We thank Drs Y. Iwakura, L. H. Glimcher, K. Nakanishi, R. D. Schreiber and Y. Fukui for providing mice and cells. We are indebted to Richard Jennings for his critical review of this manuscript.

This work was supported by Special Coordination Funds on 'Molecular Analysis of the Immune System and Its Manipulation on Development, Activation and Regulation' for Promoting Science and Technology (K.T.); by Grant-in-Aid for Scientific Research on Priority Areas and on Emerging and Re-emerging Infectious Diseases from the Japanese Ministry of Education, Science, Sports and Culture; Grant-in-Aid for Research on Emerging and Re-emerging Infectious Diseases from the Ministry of Health, Labor, and Welfare of Japan; and by Uehara Foundation.

References

1 Mosmann TR, Cherwinski H, Bond MW, Giedlin MA, Coffman RL. Two types of murine helper T cell clone. I. Definition according to profiles of lymphokine activities and secreted proteins. *J Immunol* 1986; **136**:2348–57.
2 Abbas AK, Murphy KM, Sher A. Functional diversity of helper T lymphocytes. *Nature* 1996; **383**:787–93.
3 O'Garra A. Cytokines induce the development of functionally heterogeneous T helper cell subsets. *Immunity* 1998; **8**:275–83.
4 Murphy KM, Ouyang W, Farrar JD, Yang J, Ranganath S, Asnagli H, Afkarian M, Murphy TL. Signaling and transcription in T helper development. *Annu Rev Immunol* 2000; **18**:451–94.
5 O'Shea JJ, Paul WE. Regulation of T_H1 differentiation – controlling the controllers. *Nat Immunol* 2002; **3**:506–8.
6 Murphy KM, Reiner SL. The lineage decisions of helper T cells. *Nat Rev Immunol* 2002; **2**:933–44.
7 Szabo SJ, Sullivan BM, Peng SL, Glimcher LH. Molecular mechanisms regulating Th1 immune responses. *Annu Rev Immunol* 2003; **21**:713–58.
8 Thierfelder WE, van Deursen JM, Yamamoto K *et al.* Requirement for Stat4 in interleukin-12-mediated responses of natural killer and T cells. *Nature* 1996; **382**:171–4.
9 Kaplan MH, Sun YL, Hoey T, Grusby MJ. Impaired IL-12 responses and enhanced development of Th2 cells in Stat4-deficient mice. *Nature* 1996; **382**:174–7.
10 Takeda K, Tanaka T, Shi W *et al.* Essential role of Stat6 in IL-4 signalling. *Nature* 1996; **380**:627–30.
11 Shimoda K, van Deursen J, Sangster MY *et al.* Lack of IL-4-induced Th2 response and IgE class switching in mice with disrupted Stat6 gene. *Nature* 1996; **380**:630–3.
12 Kaplan MH, Schindler U, Smiley ST, Grusby MJ. Stat6 is required for mediating responses to IL-4 and for development of Th2 cells. *Immunity* 1996; **4**:313–9.
13 Agarwal S, Rao A. Modulation of chromatin structure regulates cytokine gene expression during T cell differentiation. *Immunity* 1998; **9**:765–75.
14 Pfeiffer C, Stein J, Southwood S, Ketelaar H, Sette A, Bottomly K. Altered peptide ligands can control CD4 T lymphocyte differentiation *in vivo*. *J Exp Med* 1995; **181**:1569–74.
15 Hosken NA, Shibuya K, Heath AW, Murphy KM, O'Garra A. The effect of antigen dose on $CD4^+$ T helper cell phenotype

© 2007 The Authors Journal compilation © 2007 Blackwell Publishing Ltd,